SYNTHESIS AND CHARACTERIZATION OF TUNGSTEN CARBIDE NANOPARTICLES

Thesis submitted in partial fulfillment of the requirement for
The award of the degree of
Master of Technology
In
MATERIALS SCIENCE AND ENGINEERING

Submitted by

RAVINDER PAL SINGH
Roll No.60602012

Under
the guidance of
Dr. O.P PANDEY

School of Physics & Materials Science
Thapar University, Patiala
Patiala - 147001
June-2008

Dedicated to my Loving Parents

CERTIFICATE

This is to certify that Mr. RAVINDER PAL SINGH, Roll No. 606020l2 has worked on this thesis report as a partial fulfillment for award of the degree of MASTERS OF TECHNOLGY in Materials Science and Engineering. I certify that the matter embodied in this report is of the candidate's own record and not submitted to any other university in any part or full form for the award of such kind of a degree.

(Dr. O.P.Pandey)
Supervisor
SPMS, Thapar University
Patiala

Countersigned by:

Dr.O.P.Pandey
(Prof. & Head)
School of Physics and Materials Science
Thapar University, Patiala.

Dr. R.K.Sharma
Dean of academic Affairs
Thapar University
Patiala.

ACKNOWLEDGEMENT

Knowledge in itself is a continuous process. I would have never succeeded in completing my task without the cooperation, encouragement and help provided to me by various personalities. With deep sense of gratitude I express my sincere thanks to my esteemed and worthy supervisor, **Dr. O. P. Pandey**, Professor and Head, School of Physics and Materials Science, for his valuable guidance in caring out this work under his effective supervision, encouragement and unforgettable cooperation.

I wish to express my sincere thanks to P.G. In charge **Dr. Kulvir Singh,** Assistant Professor School of Physics and Materials Science, who have been constant sources of inspiration for me throughout this project work.

I wish to express my thanks to **Mr. Akshay Kumar**, Research Scholar without his co-operation and guidance I couldn't be able to complete my thesis work.

I would like to thank all the teaching staff for their full motivation and appreciation to my work. My thanks to P G Lab in charge **Mr. Purushottam**. His assistance and partnership were of great pleasure. His comments and views were very insightful and helpful. I would also like to thank **Mr. Jant Singh**, for providing all kind of assistance in PG Lab for creating a healthy research environment.

I would also like to give many thanks to Research Scholars **Mr.Vishal Chaudhary, Mrs. Anu Arora** and **Ms. Kamalpreet Kaur** for any kind of help and valuable suggestions whenever I needed out of their busy schedule. All my friends and my colleagues at the Materials Science & Engineering program and the School of Physics and Material Sciences are acknowledged for providing me a friendly atmosphere and encouraging me throughout this work.

I am deeply thankful to my Family, their moral support and patience has bared fruit through completion of this Thesis which will result in award of the prestigious degree of M.Tech Materials science & Engineering.

Above all I render my gratitude to the Almighty who bestowed self –confidence, ability, strength and path to me in accomplishing this work.

Ravinder Pal Singh

RAVINDER PAL SINGH

Roll No.60602012

ABSTRACT

Tungsten Carbide (WC) is one of the hardest materials used in cutting tool industry and as coating material. Fine and uniform distribution of tungsten carbide in the ductile metal matrix can give remarkable results like longer tool life. By reduction in size from micro to nano scale materials show different properties because of the high surface to volume ratio. High hardness and better toughness can be obtained by synthesizing particles of tungsten carbide in nano dimensions. Nano-grained WC/Co composites have the potential to become the new materials for tools and dies and wear parts. Shorter sintering time, high purity, and precise control of composition are the benefits of nano-grained WC/Co particles. These materials have superior properties and more homogeneous microstructure than conventional WC/Co composites. Higher toughness and ductility can be achieved without reducing hardness and wear resistance. In the present investigation thermo-chemical route for the synthesis of tungsten carbide nano particles is followed up. The synthesized powder is characterized by X-Ray diffraction and TEM technique. Thermal stability of powder is analyzed by DTA and TGA. The detail of the synthesis and characterization work is presented in this thesis.

LIST OF TABLES

LIST OF FIGURES

LIST OF ABBREVIATIONS

SEM	Scanning electron microscopy
TEM	Transmission electron microscopy
WC	Tungsten Carbide
DTA	Differential Thermal Analysis
TGA	Thermal Gravimetric Analysis
XRD	X-Ray Diffraction

CHAPTER – 1

INTRODUCTION

1.1 Introduction

Cemented tungsten carbide is one of the oldest and most successful powder metallurgy products which have its commercial applications in cutting tool industry [1]. Exceptional hardness with good wear/erosion resistance is the basic properties of WC which makes it suitable as a cutting tool substance. Cutting tools must be able to resist high temperature and severe temperature gradients, thermal shock, fatigue, abrasion, attrition, and chemical induced wear [2, 3]. Thus materials for cutting tools and dies must have high hardness to combat wear, hot strength to overcome the heat involved, and sufficient toughness to withstand interrupted cuts or vibrations occurring during the machining process. Cutting tools are a two billion-dollar industry worldwide and form the backbone of manufacturing operations for metals, polymers, and advanced materials such as intermetallics and composites of all types [2, 3].

Tungsten carbide (WC) has been well known for its exceptional hardness and wear/erosion resistance. Ductile metals, such as cobalt, which act as binder greatly, improve its toughness so that brittle fracture can be avoided. These composites are essentially aggregates of particles of tungsten carbide bonded with cobalt metal via liquid-phase sintering. The properties of these materials are derived from those of the constituents – namely, the hard and brittle carbide and the softer, more ductile binder. The cutting tool and wear part applications arise because of their unique combination of mechanical, physical, and chemical properties. Although other metal carbides, such as TiC, are also used in cutting tools, around 95% of all cemented-carbide cutting tools are tungsten carbide-based [1]. In 1992, 60% of metallic tungsten produced went into WC for cutting tools, dies, etc., only 25 % went into lamp filaments, heating elements, and mill

products, with most of the remainder was used in steels and super-alloys [4]. Annual production of tungsten for use in tungsten carbide worldwide was about 25,000 metric tons in 1991/92 [5]. The traditional method of making WC-Co cemented carbide is by crushing, grinding, blending and consolidation of the constituent powders. In this way the distribution of WC in ductile matrix find its limited approach where its size can not be reduced further as compared to the size of milled powder which is typically 1-10 micron in diameter on microscopic scale. However, efforts have been made to obtain fine distribution of WC in the ductile matrix. With great efforts, the micro structural scale can be reduced to about 500nm [4]. Nanocrystalliine ceramic materials were found to have higher hardness, fracture toughness and ductility and are sintered at lower temperature and pressure than coarse-grained powder [5]. It is therefore expected that the properties of cutting tools (to resist high temperature and severe temperature gradients, thermal shock, fatigue, abrasion, attrition and chemical induced wear) can be improved by lowering the grain size into nanoscale [6, 7].

1.2 THE DISCOVERY OF TUNGSTEN CARBIDE

Henri Moissan (1852-1907), a Nobel Laureate (1906), is best known as the inventor of electric furnace and for his unsuccessful attempts to prepare artificial diamonds. It was in the laboratory in a school of pharmacy at the University of Paris where the two carbide of tungsten were discovered namely W_2C (1896) by H. Moissan and WC (1898) by P.Williams [8]. The first commercial tungsten carbide products were melt cast for wire-drawing dies. Unfortunately, the cast pure WC was quite impractical in nature because the stiochiometric compound WC, with 6.13 weight % carbon, does not melt congruently. This decomposes to a fragile mixture of W_2C, WC and graphite upon cooling. However, at lower carbon contents, mixture of WC and W_2C are formed on cooling, which melt at a relatively moderate temperature, around 2750°C. The

resultant cast product was very hard and brittle, but very much usable for some application such as dies [8].

The first sintered tungsten carbide was produced in 1914 for use in drawing dies and rock drilling. It was developed in an attempt to avoid the casting defects common to the molten product, and consisted of powder tungsten carbide or molybdenum carbide or mixture of both, which were pressed and then sintered just below the melting temperature of the pure WC. However, the sintered product was very brittle and unsuccessful in industry for its further use [8].

1.3 TUNGSTUN CARBIDE PHASE DIAGRAM

WC is a compound comprising of W and C elements. The reaction of W with C leads to formation of several compounds. These reactions do occur at different temperatures with variation in C content. An equilibrium reaction between W and C may provide the path for formation of different phase. The existence of equilibrium phases at different composition and temperature is shown in binary phase diagram (W-C) (fig.1.1).

The binary phase diagram of W-C shows three stoichiometries, hexagonal W_2C crystallizing in three modifications, the PbO_2, Fe_2N and CdI_2 types, denoted by β, β' and β" respectively, the cubic sub-carbide WC_{1-x} crystallizing in the NaCl type structure denoted by gamma, and the hexagonal WC denoted by δ. W_2C exhibit a comparatively wide homogeneity range of 25.5 to 34 at % C at 2715°C. This phase originates from a eutectoidal reaction between elements W and δ -WC at 1250°C and melts congruently with the W solid solution at 1715± 5°C and with WC_{1-x} at approximately 2758°C [7]. Phases of W_2C stoichiometry are obtained as intermediate products during WC production. The gamma- phase results from a eutectoid reaction between β and δ at 2535°C which melts at approximately 2785°C. It can be obtained at room temperature by

extremely rapid cooling e.g. in plasma sprayed layers. The technically important δ-WC is the only binary phase stable at room temperature and has almost no solid solubility up to 2384°C but may become carbon deficient between this temperature and its incongruent melting point [8]. The monocarbide WC has a simple hexagonal crystal structure with two atoms per unit cell and a c/a ratio of 0.976 [8]. The stable structure of tungsten is body centered cubic (α-W) but a second form α-W has long been recognized which is stable at temperature below 650°C with A15 cubic structure. β-W phase was first observed in dendritic metallic deposits, formed on cathode after electrolysis of phosphates metals below 650°C [9]. Hydrogen reduction of WO_3 at T≤575°C is the most direct method of obtaining x-ray pure β-W, [10].

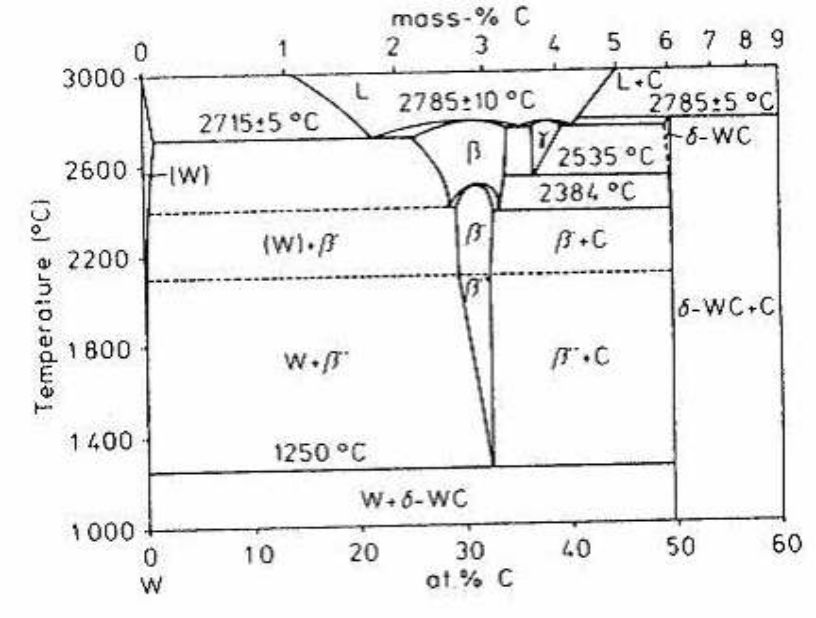

Figure1.1 Phase diagram of tungsten carbide

1.4 Cemented Carbide

Cemented tungsten carbide originated in the electric incandescent lamp industry in the US and in Germany. Since the invention of tungsten filaments for use in incandescent lamps at the beginning of the 20th century, the lamp manufacturers had been searching for a replacement for

the expensive diamond dies used in the wire-drawing of fine tungsten filaments. Prompted by a strategic shortage of industrial diamonds at the beginning of World War I, the German lamp industry turned to the tungsten carbides as potential substitute materials. Because of their extreme hardness, the carbides of tungsten initiated a substantial research and development effort on the part of the incandescent lamp industry and their suppliers, for more than two decades. A major break through took place with the advent of cemented tungsten carbide in the 1920's. The successful development of the cemented carbides was generally attributed to the work of Karl Schr'ter who was a chemist [6]. At the beginning of World War I, he began searching for substitute materials for diamond in tungsten-wire-drawing equipment, starting with cast and sintered tungsten carbides. But neither the sintering process nor the casting processes for making tungsten carbide wire-drawing dies were deemed successful and the work was abandoned. It was resumed about 1920 at Osram. Systematic experiments to bind powdered tungsten carbide with iron, nickel or cobalt were carried out from 1918 to 1923. The first sintered cemented carbide dies were prepared in 1922. The wire-drawing tests showed cobalt to be the best additive.

The invention of the cemented carbide tool materials was first disclosed in 1923 in Karl Schr ter's patent application [11]. The two inventions claimed by the patent were: a unique hard metal alloy composition, namely the combination of the very hard tungsten carbide, WC, with small amounts of a metal of the iron group: Fe, Ni and Co; and the manufacture of the hard metal alloys by the application of the process of powder metallurgy, namely the pressing and sintering of mixed powders of tungsten carbide and binder metal.

The manufacturing process, then and now, is one of powder metallurgy, with liquid phase sintering. Karl Schr'ter's "decisive step" consisted of sintering a mixture of 90 wt% tungsten carbide and 10 wt% binder metal, namely iron, nickel or cobalt, but preferably cobalt, at

temperatures at which the binder is liquid and complete consolidation of the compact occurs. The resulting microstructure consists of an aggregate of fine (1-2 micrometers) WC particles embedded in the cobalt-rich binder. The properties are controlled by composition and microstructure: the hardness increases with decreasing Co content and smaller particle size of WC, but, in general, at some cost of rupture strength and fracture toughness. The result was what we now know as "cemented carbides," a class of materials having distinctive microstructure and superior physical properties. The importance of the invention is confirmed by noting that today, seventy years later, the same compositions, made by essentially the same process, are still a very significant product of the tool materials industry. In tungsten-wire plants, the cemented carbide drawing dies quickly replaced diamond dies for reducing heated tungsten wire in the coarse range, after the swaging operation, i.e. from about 0.7 mm down to 0.3 mm in diameter. Significant as it was for wire-drawing dies, the new material represented a truly revolutionary cutting tool material for machining. The addition of cobalt to tungsten carbide not only allows the sintering of dense compacts at reasonable temperatures, but also results in materials with adequate toughness at very high hardness levels. When the new tools, made from sintered WC-Co, were placed on the market in 1927, they caused a sensation in the machine tool industry, by allowing cutting speeds 3 to 5 times faster than the best high speed steel tools in use at that time.

Modification of Schr ter's compositions by replacing either a portion or all of the tungsten carbide with other carbides (in particular those of titanium, tantalum, and molybdenum) led to the major discovery that such additions were essential for cutting steel at speeds that provide economic advantages. The discovery by Schwarzkopf that solid solutions of carbides are superior to individual carbide was the starting point of the development of multi-carbide cutting tools for high-speed machining of steel [12]. The most important advance in cutting tool

technology since the development of WC-Co was the development of coated tools in late the 60's and early 70's. Coatings are diffusion barriers, and they prevent the interaction between the chip formed during machining and the cutting material. Typical coatings are titanium carbide (TiC), titanium nitride (TiN), titanium carbonitride (TiCN), and alumina (Al_2O_3), which are extremely hard, thus very abrasion resistant. TiN has the added advantage of a significantly lower coefficient of friction against steels compared to WC/Co. Thus it reduces the energy needed during the cutting operation. All these compounds have extremely low solubility in iron and they enable inserts to cut at much higher speeds than is possible with uncoated cemented carbides. It was estimated that 80% of carbide tools sold today are coated.

1.5 PROPERTIES OF TUNGSTEN CARBIDES

The key factor for the properties of WC-Co composites are the composition and the crystal structure [1]. Deviation from the ideal composition (carbon content) leads to the occurrence of either graphite or ternary compound. Both of these are undesirable, and results in degradation of mechanical properties and cutting performance. Therefore the carbon content must be maintained with in narrow limits to obtain the desired composition with optimum properties as shown in figure (1.2). Table 1.1 presents some physical and mechanical properties of cemented carbide material.

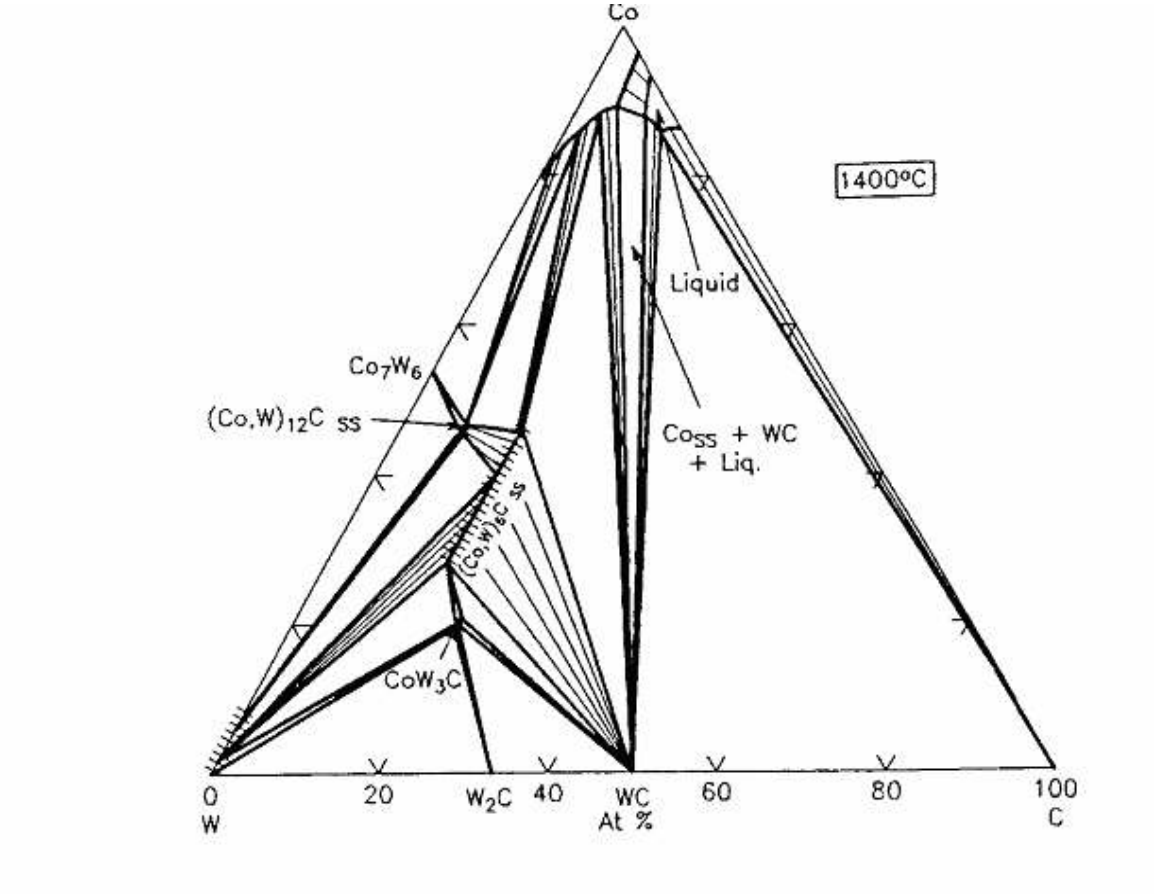

Fig 1.2 The isothermal section of WC-Co phase diagram at 1425 °C

TABLE 1.1: PROPERTIES AND REPRESENTATIVE GRADE OF CEMENTED CARBIDE, [13]

Cemented carbide	Room temperature hardness, (HV)	Modulus of elasticity, (GPa)	Transverse rupture strength, (MPa)	Coefficient of thermal expansion, (10^{-6}/K)	Thermal conductivity, (W/mK)	Density, (g/cm^3)
WC-20 wt%Co	1050	490	2850	6.4	100	13.55
WC-10 wt%Co	1625	580	2280	5.5	110	14.50
WC-3 wt%Co	1900	673	1600	5.0	110	15.25
WC10wt%Co 22wt%(Ti,Ta,Nb)C	1500	510	2000	6.1	40	11.40

Compared to other refractory carbides, the thermodynamic stability of tungsten carbide is relatively low, as is its room-temperature hardness. At high temperatures, most cubic carbides rapidly lose their hardness, whereas the hardness of the WC is quite stable. Coupled with this fact, the unique deformation characteristics of WC are the basis for its predominance as the hard refractory phase in cemented carbides. Other noteworthy properties of WC are its extremely high modulus of elasticity, second only to that of diamond, and its high thermal conductivity. The other refractory carbides have been used effectively as grain growth inhibitors in liquid phase sintering of WC-Co.

It has been found that the effectiveness of a transition metal carbide as a grain growth inhibitor is related to its thermodynamic stability, and they may be ranked as follows:

VC>Mo2C>Cr3C2>NbC>TaC>TiC>Zr/HfC

It was also found that there is a maximum level above which no further grain growth inhibition occurs. This level is believed to correspond to the maximum solubility of the carbide phase in liquid cobalt. A liquid phase that is saturated with inhibitor carbide would reduce the solubility

of WC, and thereby reduce its coarsening rate. Table 1.2 lists properties of refractory carbides and binder metals [14].

Table 1. 2. Properties of refractory metal carbides and binder materials [14].

Material	Hardness HV (50 kg)	Crystal structure	Melting temperature (°C)	Theoretical density, g/cm^3	Modulus of elasticity, GPa	Thermal expansion, μm/m•K
WC	2200	Hexagonal	2800	15.63	696	5.2
W_2C	3000	Hexagonal	2777	17.3	———	———
TiC	3000	Cubic	3100	4.94	451	7.7
VC	2900	Cubic	2700	5.71	422	7.2
HfC	2600	Cubic	3900	12.76	352	6.6
ZrC	2700	Cubic	3400	6.56	348	6.7
NbC	2000	Cubic	3600	7.8	338	6.7
TaC	1800	Cubic	3800	14.50	285	6.3
Cr_3C_2	1400	Orthor-hombic	1800	6.66	373	10.3
Co	<100	Cubic/hex agonal	1495	8.9	207	16.0
Ni	<100	Cubic	1455	8.9	207	15.0

The role of cobalt in cemented carbides is to provide a ductile bonding matrix for tungsten carbide particles. Cobalt is used as a bonding matrix because its wetting or capillary action during liquid phase sintering allows the achievement of high densities. Because of the relatively high cost of cobalt, attempts have been made to design alternate materials, with iron and nickel as the predominant cobalt substitutes. However, sliding wear tests show that cobalt content is very important for cemented carbides to have good wear resistance. Fracture in WC/Co systems with high Co contents has been found to occur mainly by the ductile rupture of Co through void nucleation and coalescence. Other fracture modes such as fracture along WC/Co interface and WC/WC grain boundary decohesion as well as cleavage across WC grains were also noted.

These mechanisms occur especially at low volume fractions of Co binder in the composite at which the contiguity of WC grains begin to increase. The effect of the contiguity of WC skeleton on fracture toughness has also been demonstrated. In a fracture toughness experiment, in a given crack plane, the crack propagation is easy along the relatively weak WC/Co and WC/WC boundaries and final fracture is primarily controlled by the area fraction of Co regions intact across the crack plane ahead of the tip. Since the WC/WC decohesion and WC/Co interface fracture energies are likely to be lower than the fracture energy absorbed in ductile fracture of the binder, ductile failure of Co can be considered as a primary mechanism manifesting the fracture resistance.

Several investigations attempted to correlate the microstructural parameters and mechanical properties of constituent phases to experimentally measured fracture toughness values. In particular, it has been universally found that the fracture toughness increases with volume fraction, the mean free path length of the binder and the size of WC grains. In addition, higher toughness has been suggested to result from the increased contiguity of Co binder, which minimizes the fracture along weak WC/WC boundaries. For a given volume fraction, geometrical arrangement of the ductile binder as a continuous thin matrix phase is beneficial for high toughness while retaining high strength. This arrangement could be most desirable of several possible arrangements in which the deformation of ductile Co phase is highly constrained in the microstructure.

1.6 Nano Particle Materials Research:

Nanoscale particle research has recently become a very important field in materials science. Nanoscale particles (1 to 100 nm) usually have physical properties different from those of large particles (10-100 nm) or the molecular/atomic species. It has been found that nanoparticles exhibit a variety of previously unavailable properties, depending on particle size, including magnetic, optical, and other physical properties as well as surface reactivity [15]. Recent experiments have shown that consolidated nano-materials have improved mechanical properties, such as increased hardness of metals and increased ductility and plasticity of ceramics. The unique properties of nanoscale particles and nanograin bulk materials can be attributed to two basic phenomena. The first is that the number of atoms at the surface and/or grain boundaries in these materials is comparable to that of the atoms located in the crystal lattice, thus the chemical and physical properties are increasingly dominated by the atoms at these locations. The second phenomenon is the "quantum-size effect" or quantum confinement effect. When particles approach the nanometer size range, their electronic and photonic properties can be significantly modified as a result of the absence of a few atoms in the lattice and the resulting relaxation of the lattice structure. The worldwide cemented carbide cutting tool industry has approached the problem of higher mechanical properties for their cutting tools by altering composition primarily in the direction of increased carbide content. Unfortunately, at the level of 94 to 97 weight percent carbides, fracture toughness and strain tolerance have fallen below acceptable levels and excessive brittleness results. One answer to this dilemma is to reduce the average particle size of the hard carbides, thus reducing the mean free path between carbide particles. This usually has the effect of increasing fracture toughness as well as wear resistance. The latter effect is achieved because the matrix is now exposed to the abrasive/corrosive environment over much smaller dimensions, even though the WC/Co composition has not changed. By means of this particle size

reduction process, the fracture toughness and strength can be increased significantly, as long as two other deleterious effects have not been introduced. These are:

- Excessive impurities such as oxygen during the very long milling times necessary for mechanical mixing, and
- Establishment of WC-WC particle contact, especially over distances spanning many WC particles, thus creating a brittle fracture initiation site and propagation path. These two problems will negate any increase in fracture toughness in other portions of the volume of the tool.

These effects limit the cost-effective mechanical milling reduction of particle size and proper WC/Co dispersion to a typical average WC size of 0.5 to 1.0 micron. The most striking is the abrasion resistance, with finer grain composites (still in micron range) having much better abrasion resistance.

1.7 Applications

Cemented carbides, best known for their superior wear resistance, have a range of industrial uses which are diverse compared to other powder metallurgy product applications. Common uses include metalworking tools, mining tools, and wear resistant components. All of these applications have one physical property requirement in common: the ability to resist wear. The performance of cemented carbide as a cutting tool lies between that of tool steel and “cermets” [20]. Compared to tool steels, cemented carbides are harder and more wear resistant, but also exhibit lower fracture resistance and thermal conductivities than tool steel. Cermets, which are composed of carbonitride based materials such as TiCN, on the other hand are more wear

resistant than cemented carbides, but may not be as tough. Advances in cemented carbides have produced a wide selection of tool materials. They are suitable to cut a variety of materials such as gray cast iron, ductile nodular iron, austenitic stainless steel, nickel-base alloys, titanium alloys, aluminum, free-machining steels, plain carbon steels, alloy steels, and martensitic and ferrite stainless steels. Almost 50% of the total production of cemented carbides is now used for nonmetal cutting applications such as drill bits and components for mining, oil and gas drilling, transportation and construction, metalforming, structural and fluid-handling components, and forestry tools [20]. New applications are constantly being identified for carbides, largely because of their excellent combinations of abrasion resistance, mechanical impact strength, compressive strength, high elastic modulus, thermal shock resistance, and corrosion resistance. Erosion resistance of carbides is important in applications such as sand blast/spray nozzles, seals in slurry pumps, and component parts in the oil industry. Cemented carbide is an excellent choice for the nozzles because it can outwear steel 100 to 1 and will thereby maintain the spray pattern and quantity of flow for a longer period of time, extending the service life of the nozzles. Many applications can use a small carbide nozzle insert held to other base materials by epoxy, braze, and shrink fit or taper fit. This permits the use of carbide without a major redesign of a nozzle assembly or the need to manufacture a complex shape from solid carbides. In the mining and mineral industries, the components exposed to severe mechanical interaction among very abrasive nonmetallic and metallic materials. The abrasive nature of most ores can cause significant wear to both handling and processing equipment. A variety of WC/Co materials have been used for hard facing to meet an extremely wide range of severe abrasive conditions, especially oil well drill bits, tool joints, rock drill bits. The physical and mechanical properties of cemented tungsten carbides make them appropriate materials for a wide range of structural

components, including plungers, boring bars, powder compacting dies and punches, high pressure dies and punches, pulverizing hammers, carbide feed rolls and chuck jaws, and many others. The predominant wear factors in most applications are high abrasion, attrition, and erosion. The rigidity, hardness, and dimensional stability of cemented carbide, coupled with its resistance to abrasion, corrosion, and extreme temperature, provide superior performance in fluid-handling application, such as seal rings, bearings, valve stems, and valve seats. Among the diverse applications of cemented carbides is a wide range of tools and components for the transportation and construction industries. Examples include tools for road planing, soil stabilization, asphalt reclamation, vertical and horizontal drilling, trenching, dredging, tunnel boring, and forestry, as well as snow-plow blades, tire studs, and street sweeper skids. Erosion resistance of carbides is important in applications such as sand blast/spray nozzles, seals in slurry pumps, and component parts in the oil industry. The success of cemented carbides in erosion-resistant application is again due to their unique composite structure of wear-resistant WC particles in a ductile cobalt matrix. WC-Co has also been used as coatings in jet engine parts such as fans and high pressure compressors (HPC). The materials used for fan and HPC blade interlocks in a jet engine are usually titanium alloys, which have poor wear properties. Most fan and HPC interlocks use thermal sprayed WC-Co coatings or brazed-on WC-Co powder metallurgy wear pads to prevent excessive wear. The WC-Co coatings are successful in the titanium alloy interlock applications because of the following reasons.

- High wear resistance of the tungsten carbide,
- Adequate fracture toughness because of the cobalt matrix,
- High adherence on the titanium alloy substrates, and

- Good match in coefficient of thermal expansion with the titanium alloy substrate materials.

The typical range of temperatures for fan interlocks is from subzero to 95 ^{o}C in the fan and from 40 to 260^{o}C in the HPC. Fortunately, WC-Co coatings appear to retain sufficient low-temperature ductility and high temperature oxidation resistance over these temperature ranges. The formation of a wear glaze at the contact zones contributes to the good wear resistance of the WC-Co in the interlock applications. The WC-Co coatings have also been used in other engine components such as nozzle assemblies. The titanium components in the exhaust nozzle generally have poor wear resistance and almost always require coatings on mating parts in relative motion. Oxidation of the carbide limits use of this coating to temperatures below 480 ^{o}C. Nano grained WC/Co composites are expected to enter the above mentioned areas. With both high hardness and high toughness, new applications for nano grained WC/Co composites are also expected to be found.

CHAPTER – 2

LITRATURE REVIEW

McCandlish L.E., Kear B.H. and Kim B.K **[22]** reported the thermo chemical synthesis method of WC-Co nanoparticles. With traditional methods of synthesis WC embedded in cobalt matrix typically (1-10μm) sized particles can be achieved. To reduce the particle size to nano scale one of the initial methods was thermo chemical synthesis method. In this approach one has to start with a precursor compounds in which W and Co are mixed at the molecular level, and then to transform these compounds into nanostructured WC-Co powder by thermo chemical treatment. Various steps followed in thermo chemical synthesis are:

- Precipitation of molecular precursor powder (W_3O) at 100°C thereby mixing W and Co at molecular level.
- Reacting precursor powder at controlled carbon and oxygen activity at 600 to1000°C to produce nano structured WC-Co powder.
- Addition of lubricant and to press to shape by cold compaction.
- HIP- sinter at 1200°C.

A prerequisite is a homogeneous precursor powder, in which W and Co are intimately mixed at molecular level, such as in the compound tris(ethylenediamine) cobalt tungstate, $Co(en)_3WO_4$, which after reduction and carburization yields WC-23wt% cobalt . Other composition (i.e. W/Co ratios) can be obtained from aqueous solution mixture, such as $Co\ (en)_3WO_4 + H_2WO_4$ or AMT

+ $CoCl_2$ (where AMT= $(NH_4)_6(H_2W_{12}O_{40}).4H_2O$. These solution, upon atomization and rapid drying, precipitate homogeneous powder with amorphous or microcrocrystalline structure, which are suitable precursors for subsequent thermo chemical processing to the desired nanostructure WC-Co powder. Spray dried powders have been used to produce WC-Co powders with from 3-30 wt % Co. Reduction of Co $(en)_3WO_4$ powder in 1:1 H_2: Ar gas, as the powder is heated from room temperature to 700°C at the rate of 25°C / min. The ethylenediemine ligands are cleanly removed at between 150-250°C and reduction is complete at 650°C. The result of this reduction process is a nanostructured powder. Consolidation of powder is done by liquid phase sintering. However, it is necessary to minimize the time spent at the sintering temperature in order to minimize particle coarsening; tests have shown that dense structures in WC-Co Wt% Co can be achieved in 30 seconds at 1400°C which gives WC grain size of about 200nm. An additional 30 second sintering time increase the WC grain size to 2.0 microns. A small amount of uncombined C or an addition of Cr inhibits grain growth during liquid phase sintering. Ultra pure WC-Co powders can be consolidated by solid state sintering, where grain growth is much slower. Critical to the success of the process is the control of thermodynamics and kinetics of gas-solid reactions in a field bed reactor. A low sintering temperature and a short sintering time insure reaction of a nanostructure in consolidated material.

Zhu Y. T. and Manthiram A **[23]** reported the synthesis of WC-Co nano composite from ammonium tungstentate using a polymer as carbon source. Use of a polymer as an in situ carbon source reduces the diffusion length and become particularly attractive for large scale production. Procedure involve the mixing of ammonium tungunstate and cobalt nitrate, decomposition in air on a hot plate, dispersion in a dimethylformamide (DMF) solution of polyacrylonitrile and firing in Ar-H_2 mixture at 800-900°C which yield WC. Addition of aqueous cobalt acetate in it and

evaporating the solvent we get a black mass which fired at 400°C for 4 hour in a mixture of 90% Ar-10% H_2 gives the final product.

Fig 2.1 Synthesis of WC-Co nano composite using polymer as carbon source

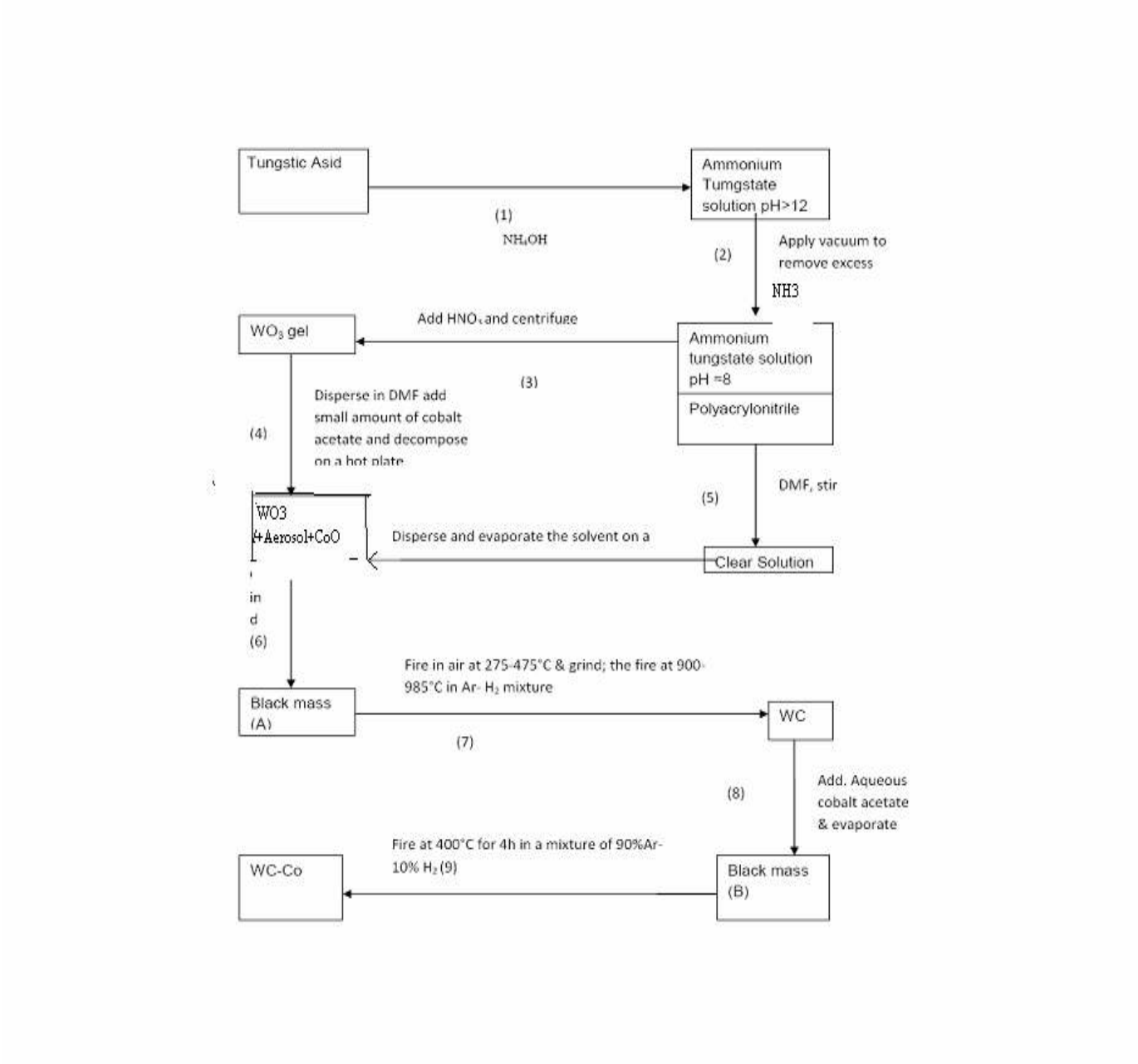

Geo L. and. Kear B.H **[24]** studied the synthesis of nanophase WC powder by a displacement reaction process**.** It is a novel displacement reaction process which combines reduction and

carburization of ammonium or tungsten oxide in a single operation. The critical step in the process is the heating rate, which should be slow enough to ensure a balance between reduction and carburization kinetics. The process is a one step process, a gas phase mixture of H_2/Co (2:1) or (1:1 molar ratio) is passed over the heated tungsten base precursor powder at temperature up to 700°C in order to affect its direct conversion to nanophase WC.

Fig 2.2 Synthesis of nanophase WC powder by displacement reaction.

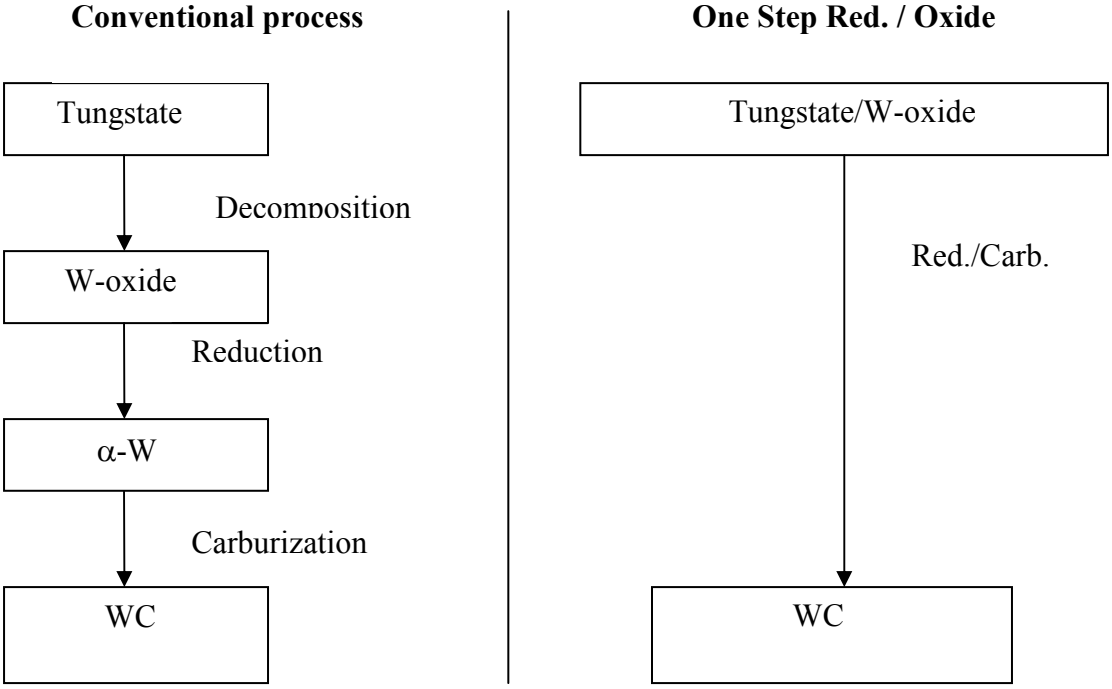

The proposed displacement reaction process involving the formation of an intermediate oxy-carbide phase. The initial nanophase tungsten oxide particle is reduced by H_2 through the formation of H_2O at its surface. As the H_2O molecules are removed by the flowing gas stream, the active tungsten sites react with the Co to form an incipient oxy-carbide phase, liberating CO_2 that is also carried away by the flowing gas stream. Further reaction gradually transforms the oxy-carbide into nanophase WC. In this case the formation of metastable W_2C phase is avoided.

BAN Z. G. and Shaw L.L.,**[25]** reported the synthesis of nanostructured WC-Co powder by integrated mechanical and thermal activation(IMTA) process. As a result of integrated mechanical and thermal activation (IMTA), nanostructured WC-Co powder is synthesized below 1000°C starting from WO_3, CoO and graphite powder mixture. Consolidation of nanostructured WC-Co powder is done via. High velocity oxy-fuel (HVOF) thermal spraying and solid state sintering .The powder mixture prepared containing WO_3, C and CoO with a molar ratio of 1:2.4:0.7 in order to form the final product of WC+18 wt. % Co+5.3 wt. %C. This powder mixture was high energy milled for different times.

The mechanically activated (high energy ball milled) powder was subsequently subjected to thermal activation. The thermal activation was carried out by heating the milled powder at 650°C for 2h in a gas mixture of H_2 (P_{H2}=0.5 atmosphere) and Ar (P_{Ar}=0.5 atmosphere), followed by ramping to 1000°C and holding at this temperature for 2 h in pure argon (P_{Ar}=1 atmosphere), free carbon is often present in the nanostructured WC-Co powder obtained from the IMTA process because of the extra carbon added in the beginning of the process. To control the free carbon concentration in the gas synthesized WC-Co powder, a gas mixture of CO/CO_2 was used to purify the powder at a chosen temperature after thermal activation. Consolidation of the resulting nanophase WC-Co powder is done by high velocity oxy fuel (HVOF), thermal spraying and free sintering to prepare coating and bulk samples respectively. Sintering of WC-Co is highly affected by carbon content. By using the CO/CO_2 treatment, the concentration of free carbon in the nano powder has been kept bellow 0.05wt. %, . The resulting powder has a narrow particle size distribution (0.3 to 0.5 μm) and the crystal size of the WC phase is about 30nm.

Fig 2.3 Synthesis of nanostructured WC-Co powder by integrated mechanical and thermal activation (IMTA) process

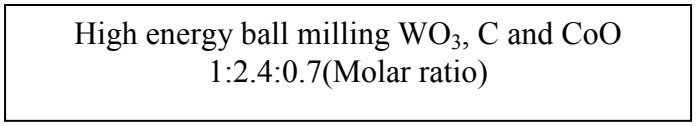

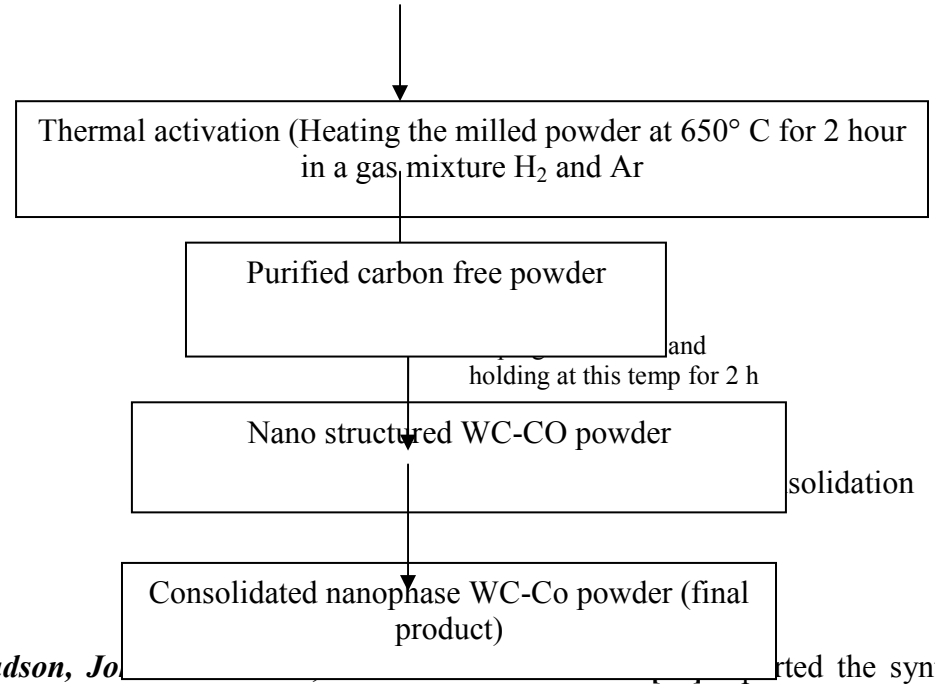

Michael J. Hudson, Jo rted the synthesis of ordered nanoparticles of WC via. low temperature SOL-GEL . Tungsten carbide particles have been prepared by the gel precipitation of tungstic acid in the presence of an organic gelling agent 10% ammonium poly (acrylic acid) in water.

Fig 2.4 Synthesis of nanoparticles of WC via low temp. SOL-GEL method

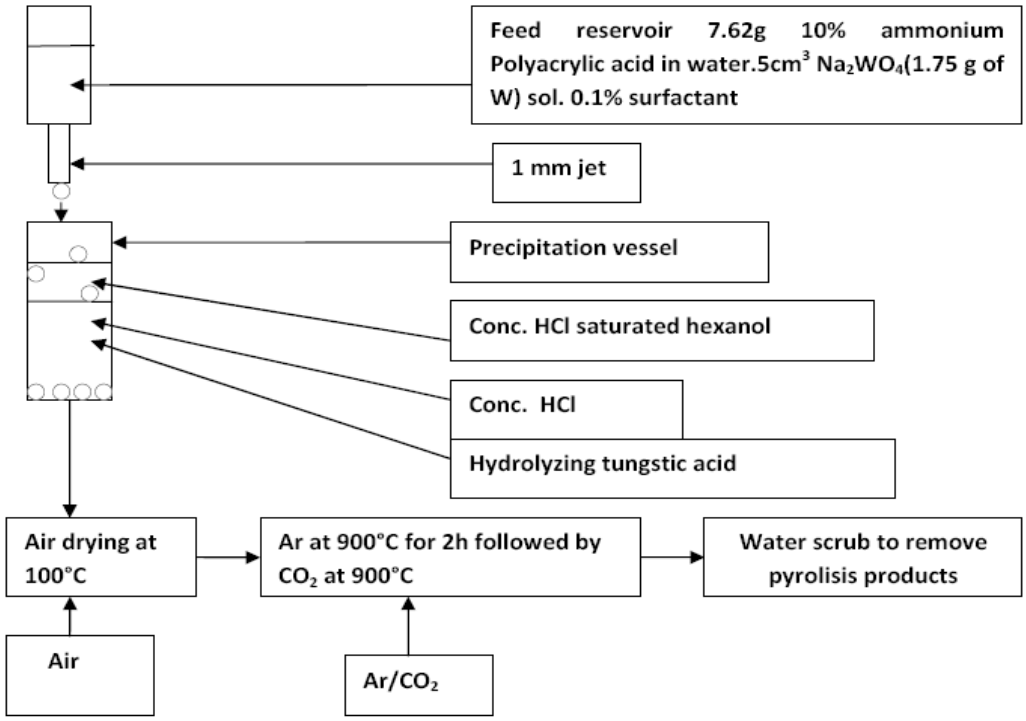

The feed solution, a homogeneous of sodium tungstate and ammonium poly(acrylic acid) in water, was dropped from a 1mm jet into hydrochloric acid saturated hexanol/concentrated hydrochloric acid to give particles of mixture of tungstic acid and poly(acrylic acid) which after drying in air at 100°C and heating to 900°C in argon for 2 h, followed by heating in carbon dioxide for a further 2 h and cooling, gives a mixture of WO_x, WC and traces of Na_xWO_3 with the carbon for the formation of WC being provided by the thermal carbonization of poly(acrylic acid). A flow sheet of the process is presented in the figure .The product after solidification for 40 min in water, consists of mainly nanoscopic tungsten carbide with a particle size of <40 to 75 nm.

Jadambaa Temuujin, Mamoru Senna, Tsedev Jadambaa and Dondog Byambasuren. **[27]** reported the synthesis of tungsten carbide nanoparticles by mechanically assisted carbothermic reduction natural wolframite. Carbothermic reduction of natural wolframite ($FeWO_4$) to nano sized tungsten carbide (WC) particles were achieved by calcining mechanically activated

mixture of $FeWO_4$ and active carbon at 1100°C under flowing argon gas. The average particle size ranged between 20 to 25nm. Intermediate, Fe_6W_6C and Fe_3W_3C, were observed between 900°C and 1100°C, which decomposes to give the final product, WC. Increased homogeneity with associated decrease in the diffusion path by milling are mainly responsible for the successful production of WC. The starting material FeWO4 (WO_3:71.85, Fe2O3:20.36, MnO2:5.46, SiO2:1.1wt %) was ball milled to reduce particle size to 10μm. Active carbon with there average particle size 35nm is used here. The composition of the mixture was set equal to the stoichiometry of the reaction;

$$FeWO_4 + 5C \rightarrow Fe + WC + 4CO$$

Well dispersed tungsten carbide nanoparticles of 20-25 nm were obtained from a direct carbothermic reduction from mechanically activated and homogenized mixtures comprising natural $FeWO_4$ and active carbon. The final product, WC, was formed via intermediate ternary carbide phases,Fe_6W_6C and Fe_3W_3C. The well-crystallized WC contained only small fractions of impurities, i.e.,Fe_3W_3C, Fe_7W_6 , W, Fe_3C, and Fe. Milling just for 2 h was sufficient for practical full conversion to WC at temperature as low as 1100°C.

***Chunli Guo, Lio Yi, Xiaojian Ma, Yitai Qian, and Liqiang Xu*[28]** reported the synthesis of tungsten carbide nanocrystals via a simple reductive reaction. Tungsten carbide nanocrystals had been prepared by the simple reaction of WO_3, Mg and anhydrous CH_3CH_2OH in an autoclave at 600°C. CH_3CH_2OH and WO_3 were used as carbon and tungsten source and Mg as the reductant. The overall reaction equation;

$$WO_3 + CH_3CH_2OH + 4Mg \rightarrow WC + C + 4MgO + 3H_2$$

Approximate amounts of WO_3 (1.5g), Mg (1g) and anhydrous CH_3CH_2OH (12ml) were put in to a stainless steel autoclave of 16ml capacity. Then the autoclave was sealed and put into an

electric furnace at 100°C, the temperature of the furnace was increased to 600°C in 50 min and maintained at 600 °C for 15 hour. Then, it was allowed to cool down to room temperature. The dark solid powder was collected and washed by dilute HCl to remove un reacted Mg powder. After that, the obtained sample was washed with distilled water and ethanol to eliminate by-products, and then it was dried in a vacuum at 50°C for 10 hour.

Viewing the literature, we got several methods for the synthesis of WC-Co nanocomposites. The method "Thermo chemical Synthesis" is used for commercial production of nanostructured WC-Co composites. The benefit of the process is, low sintering temperature and short sintering time which ensures retention of nanostructure in the consolidated material. Additional 30 second's sintering time increase the WC grain size from nano scale to micro scale.

The second method is very sensitive to production parameters; for example

- The initial mixing of ammonium tungstate and cobalt nitrate leads to the formation of $CoWO_4$ which can facilitate the formation of unwanted Co_6W_6 phase and
- The thermal degradation of polyacrylonitrile occurs over a range of temperature and is complex, which makes the firing temperature and time very critical in obtaining the desired product.
- Large quantity of sample leads to slower WC formation kinetics.

Third process is one step process which is advantageous but the limitation of this synthesis process is its heating rate which should be slow enough to ensure balance between reduction and carburization kinetics.

In IMTA process we can synthesize nanostructured WC-Co powder below 1000°C. Limitation of the process is the free carbon present in the bulk cemented carbide which reduces hardness and wear resistance, so here we have to utilize gas mixture of CO and CO_2 to control the amount of free carbon.

With "low temperature Sol- Gel Preparation method" also we can prepare nanostructured WC-Co below 1000°C. The main limitation of this process is that we have to handle the product very carefully while maintaining an atmosphere of CO_2; we have to cool it to room temperature because even if slightly warm the material gets red hot.

"Carbothermic reduction of natural Wolframite" is although a good method for the synthesis of nanostructured WC-Co but it is a high temperature synthesis method. WC particles were activated by calcining mechanically activated mixture of $FeWO_4$ and active carbon at 1100°C under flowing Argon gas.

The synthesis of WC-Co nano crystals via a simple reductive reaction is the best method among all the methods we can synthesis WC-Co nano crystals at 600°C. This synthesis route was very simple and easy to control and can be extended to synthesis other transition metal carbide.

CHAPTER – 3

EXPERIMENTAL WORK

3.1 Methodology

Experiments were performed with different carbon sources (Ethanol and Benzene).

In the first experiment WO_3 (2 g) and anhydrous CH_3CH_2OH (30-mL) were used as tungsten and carbon source respectively whereas Mg powder (8 gm) was used as reductant. The overall reaction equation could be formulated as follows:

$$WO_3 + CH_3CH_2OH + 4Mg \rightarrow WC + C + 4MgO + 3H_2 \qquad (1)$$

All the reactants were put in specially designed autoclave. Then, the autoclave was sealed and put into a resistance heating furnace. The temperature of the furnace was increased to 600ºC in 2 hours and maintained at 600ºC for 15 hours. Then, it was allowed to cool down to room temperature. The dark solid powder was collected and dissolved in HCl (1:3) to remove unreacted Mg powder. After x-ray diffraction it was found that a large amount of carbon, unreacted WO_3 and $MgCO_3$ phases were also present along with WC phase.

Further acid treatment (1:1 HCl) was done to remove these unwanted phases. The as prepared sample was again washed with ethanol and characterized using XRD, TEM and DTA.

The chemical reactions contained in the whole process could be formulated as follows:

$$Mg + CH_3CH_2OH \rightarrow MgO + 2C + 3H_2$$
$$Mg + WO_3 \rightarrow W + MgO$$
$$2W + C \rightarrow W_2C$$
$$W_2C + C \rightarrow 2WC$$
$$W + C \rightarrow WC$$

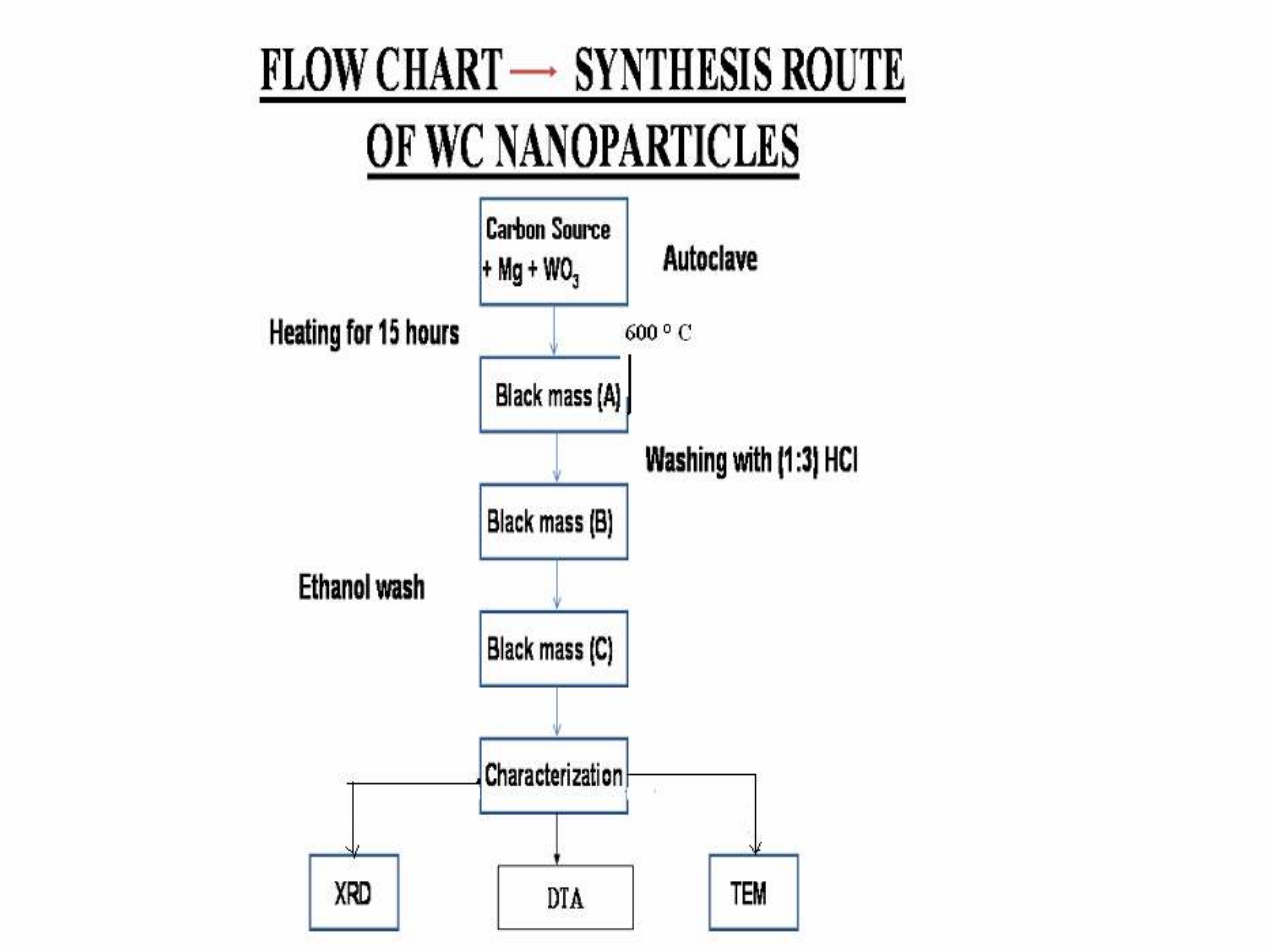

The overall reaction is formulated as:

$$WO_3 + CH_3CH_2OH + 4Mg \rightarrow WC + C + 4MgO + 3H_2$$

In the second experiment aromatic compound of carbon was tested as carbon source and the whole experiment was repeated. The reaction would be incomplete and WC phase was not formed if the reaction time was shorter than 13 hours.

3.2 CHARACTERIZATION TECHNIQUES

The characterization of tungsten carbide nanoparticles synthesized by simple reductive reaction method was carried out with various characterization methods as follows:

3.2.1 X-Ray Diffraction Studies (XRD)

X-ray diffraction is the most wide spread technique for determining the phase identification, crystal structure, lattice parameter of the crystalline solids. A typical powder XRD instrumentation consist of four main components such as X-ray source, specimen stage, receiving optics and X-ray detector as shown in fig. The source and detector with its associated optics lie on the circumference of focusing circle and the sample stage at the centre of the circle. The angle between the plane of the specimen and the X-ray source is θ, known as Bragg's angle and the angle between the projection of X-ray and the detector is 2θ. For the XRD analysis, fine powder samples were mounted on the sample holder and the powder was assumed to consist of randomly oriented crystallites. When a beam of X-ray is incident on the sample, X-rays are scattered by each atom in the sample. If the scattered beams are in phase, these interfere constructively and one gets the intensity maximum at that particular angle. The atomic planes from where the X-rays are scattered are referred to as 'reflecting planes'

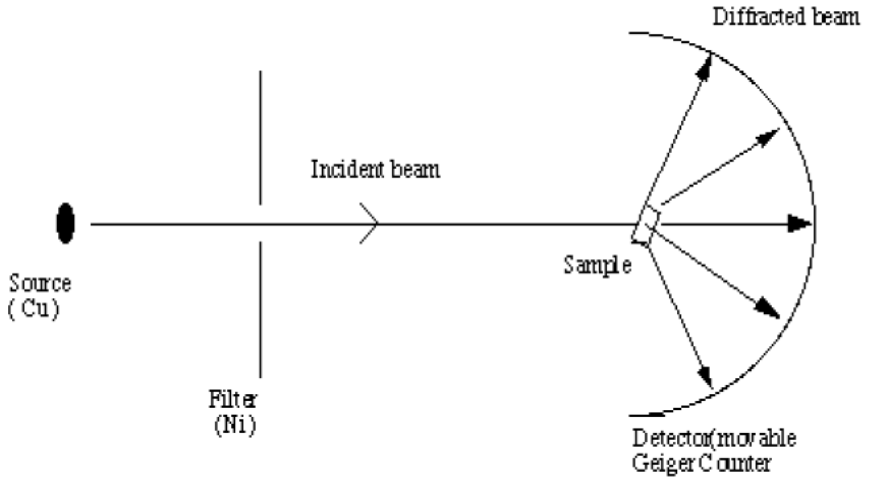

Fig 3.1 X-ray Scattering

The Bragg's law relates the wavelength (α) of the X-ray reflected the spacing between the atomic planes (d) and the angle of diffraction (θ) as follows:

$$2d \sin \theta = n \lambda$$

.For the first order diffraction, n=1, and knowing θ andλ, one can calculate the interplanar spacing d–value for a particular plane. After recording the X-ray diffraction pattern, first step involves the indexing of XRD peaks. The indexing means assigning the correct Miller indices to each peak of the diffraction pattern. The correct indexing is done only when all the peaks in the diffraction pattern are accounted for the process.

There are three main methods for indexing a diffraction pattern,

(i) Comparing the measured XRD pattern with the standard data base (JCPDS-cards)

(ii) Analytical methods

(iii) Graphical methods.

In case of fine particles, with reduction in the size of the particles, the XRD lines get broadened, which indicates clearly that particle size has been reduced. Information of the particle size is obtained from the full width at half maximum (FWHMs) of the diffraction peaks. The FWHMs (β) can be expressed as a linear combination of the contributions from the strain (ε) and particle size (*L*) through the following relation:

$$\beta \cos\theta/\lambda = 1/L + \varepsilon \sin\theta/\lambda$$

3.2.2 Transmission electron microscope

Transmission electron microscopy (TEM) is used to obtain information from samples that are thin enough to transmit electron. In TEM, the whole area of observation is illuminated using an electron source of adequate intensity. The transmitted electrons are generally used to form either an image or a diffraction pattern of the specimen .The formation of image and electron diffraction in TEM can be understood from schematic ray diagram as shown in fig.3.2

When a crystal of lattice spacing 'd' is illuminated with electrons of wavelength 'λ', the diffracted waves will be produced at specific angles 2θ for n =1, satisfying the Bragg's condition

$$2d \sin\theta = n\lambda$$

The diffracted waves form diffraction spots on the back focal plane. In an electron microscope, the use of electron lenses allows the regular arrangement of diffraction spots to be projected on a

screen and the electron diffraction pattern can be observed. If the transmitted and the diffracted beam interfere on the image plane, a magnified image can be observed. The space where the diffraction pattern forms is called the reciprocal space, while the space at the image plane or at a specimen is called the real space.

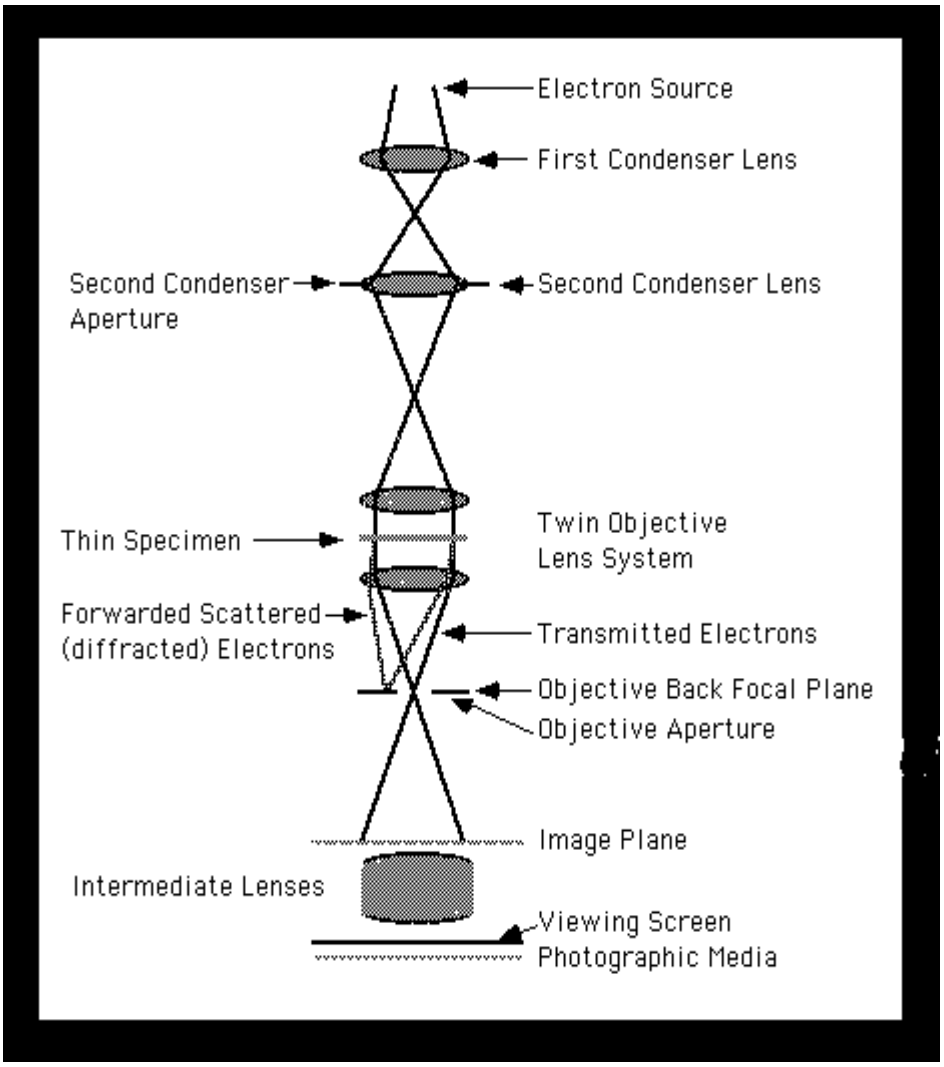

Fig 3.2 Schematic ray diagram of TEM

In TEM, by adjusting the electron lenses, both the microscope images and diffraction patterns can be observed. Thus in the analysis of microstructures of materials, both observation modes can be successfully combined. In an investigation of electron diffraction pattern, the electron microscope images of the nano phosphor is first observed of the whole area and then by inserting an aperture in a specific area and adjusting the electron lenses a diffraction pattern of the area is obtained. The latter observation mode is called selected area electron diffraction (SAED). Because a selected area diffraction pattern can be obtained from each grain, the crystal structure

and mutual crystal orientation relationship between adjacent grains can easily be clarified. The observational dimension selected from the object is usually limited to about 0.1 micrometer in diameter. However, in micro diffraction method, the diffraction pattern can be obtained from an area correspondingly to only a few nanometers in diameter. Then, by passing the transmitted beam or one of the diffracted beams through an aperture and changing to the imaging mode, the image with enhanced contrast can be observed. The observation mode using the transmitted beam is called the bright field method, and the image observed is a bright field image. When one of the diffracted beams is selected the observation mode is called as dark field method, and the image observed is a dark field image.

3.2.3. Differential Thermal Analysis (DTA)

Differential thermal analysis (or **DTA**) is a thermo analytic technique, similar to differential scanning calorimetry. In DTA, the material under study and an inert reference are heated (or cooled) under identical conditions, while recording any temperature difference between sample and reference. This differential temperature is then plotted against time, or against temperature (DTA curve or thermo gram). Changes in the sample, either exothermic or endothermic, can be detected relative to the inert reference. Thus, a DTA curve provides data on the transformations that have occurred, such as glass transitions, crystallization, melting and sublimation. The area under a DTA peak denotes the enthalpy change and it is not affected by the heat capacity of the sample. DTA involves heating or cooling a test sample and an inert reference under identical conditions, while recording any temperature difference between the sample and reference. This differential temperature is then plotted against time, or against temperature. Changes in the sample which lead to the absorption or evolution of heat can be detected relative to the inert reference. Differential temperatures can also arise between two inert samples when their response to the applied heat-treatment is not identical. DTA can therefore be used to study thermal properties and phase changes which do not lead to a change in enthalpy. The baseline of the DTA curve should then exhibit discontinuities at the transition temperatures and the slope of the curve at any point will depend on the micro structural constitution at that temperature.

A DTA curve can be used as a finger print for identification purposes, for example, in the study of clays where the structural similarity of different forms renders diffraction experiments

difficult to interpret. The area under a DTA peak can be to the enthalpy change and is not affected by the heat capacity of the sample. DTA may be defined formally as a technique for recording the difference in temperature between a substance and a reference material against either time or temperature as the two specimens are subjected to identical temperature regimes in an environment heated or cooled at a controlled rate.

The key features of a differential thermal analysis kit are as follows (Fig.3.3):

- Sample holder comprising thermocouples, sample containers and a ceramic or metallic block.

- Furnace.

- Temperature programmer.

- Recording system.

The last three items come in a variety of commercially available forms and are not being discussed in any detail. The essential requirements of the furnace are that it should provide a stable and sufficiently large hot-zone and must be able to respond rapidly to commands from the temperature programmer. A temperature programmer is essential in order to obtain constant heating rates. The recording system must have a low inertia to faithfully reproduce variations in the experimental set up.

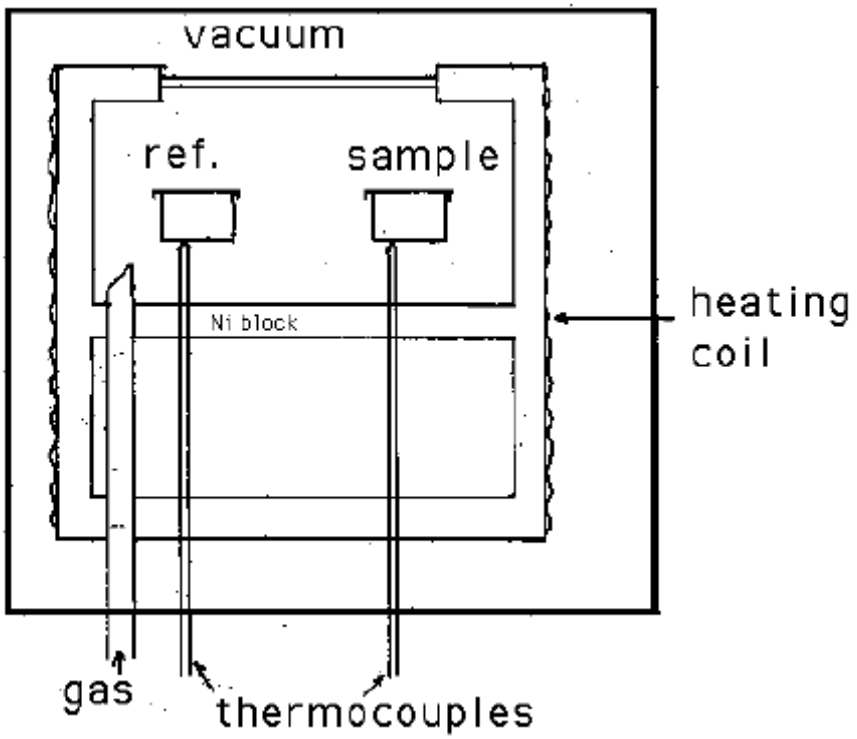

Fig 3.3: Schematic illustration of a DTA cell.

The sample holder assembly consists of a thermocouple each for the sample and reference, surrounded by a block to ensure an even heat distribution. The sample is contained in a small crucible designed with an indentation on the base to ensure a snug fit over the thermocouple bead. The crucible may be made of materials such as Pyrex, silica, nickel or platinum, depending on the temperature and nature of the tests involved. The thermocouples should not be placed in direct contact with the sample to avoid contamination and degradation, although sensitivity may be compromised.

Metallic blocks are less prone to base-line drift when compared with ceramics which contain porosity. On the other hand, their high thermal conductivity leads to smaller DTA peaks. The sample assembly is isolated against electrical interference from the furnace wiring with an earthed sheath, often made of platinum-coated ceramic material. The sheath can also be used to contain the sample region within a controlled atmosphere or a vacuum. During experiments at temperatures in the range 200 to 500°C, problems are encountered in transferring heat uniformly away from the specimen. These may be mitigated by using thermocouples in the form of flat

discs to ensure optimum thermal contact with the now flat- bottomed sample container, made of aluminum or platinum foil. To ensure reproducibility, it is then necessary to ensure that the thermocouple and container are consistently located with respect to each other. The effects of specimen environment, composition, size and surface-to-volume ratio all affect powder decomposition reactions, whereas these particular variables may not affect solid-state phase changes. Experiments are frequently performed on powders so the resulting data may not be representative of bulk samples, where transformations may be controlled by the build up of strain energy. The packing state of any powder sample becomes important in decomposition reactions and can lead to large variations between apparently identical samples. In some circumstances, the rate of heat evolution may be high enough to saturate the response capability of the measuring system; it is better then to dilute the test sample with inert material. For the measurement of phase transformation temperatures, it is advisable to ensure that the peak temperature does not vary with sample size. The shape of a DTA peak does depend on sample weight and the heating rate used. Lowering the heating rate is roughly equivalent to reducing the sample weight; both lead to sharper peaks with improved resolution, although this is only useful if the signal to noise ratio is not compromised. The influence of heating rate on the peak shape and disposition can be used to advantage in the study of decomposition reactions, but for kinetic analysis it is important to minimize thermal gradients by reducing specimen size or heating rate.

A simple DTA curve may consist of linear portions displaced from the abscissa because the heat capacities and thermal conductivities of the test and reference samples are not identical, and of peaks corresponding to the evolution or absorption of heat following physical or chemical changes in the test sample. There are difficulties with the measurement of transition temperatures using DTA curves. The onset of the DTA peak in principle gives the start-temperature, but there may be temperature lags depending on the location of the thermocouple with respect to the reference and test samples or the DTA block. It is essential to calibrate the apparatus with materials of precisely known melting points.

CHAPTER – 4

Results and Discussions

4.1 X-Ray Diffraction Analysis

Samples were characterized by X-ray powder diffraction (XRD), CuĶα radiation (λ=1.5443A˚). The final X-Ray Diffraction pattern of sample 1 shows the peaks of WC, C, $MgCO_3$ and WO_3 phases. Sample 2 also exhibit similar peaks with increased intensity of WC phase whereas intensity of all the other phases decreases. There is not any shifting in the position of the peaks. The spectrum in Fig. 4.1 shows the diffraction spectrum of sample 1(leaching with 1:3 HCl), all proposed phases are shown in this diffraction pattern. The two reflection peaks at 2θ = 35.72°, and 2θ = 48.42° corresponds to [100] and [101] planes of WC. The other two small intensity peaks at 2θ = 31.58° and 63.44° corresponds to [001] and [111] planes of hexagonal WC. The lattice parameters were calculated using equation given below:

$$d_{h,k,l}=\{4/3\ h^2+hk+k^2/a^2+l^2/c^2\}^{-1/2}$$

The as calculated lattice parameters a = 2.860 Å, c = 2.823 Å were very close to the reported value of hexagonal WC (a = 2.906 Å, c = 2.837 Å, JCPDS Card No. 51-0939).

Information of the particle size is obtained from the full width at half maximum (FWHMs) of the diffraction peaks. The FWHMs (β) can be expressed as a linear combination of the contributions from the strain (ε) and particle size (*L*) through the following relation:

$$\beta\cos\theta/\lambda=1/L+\varepsilon\sin\theta/\lambda$$

And the calculated average particle size is about 58 nm

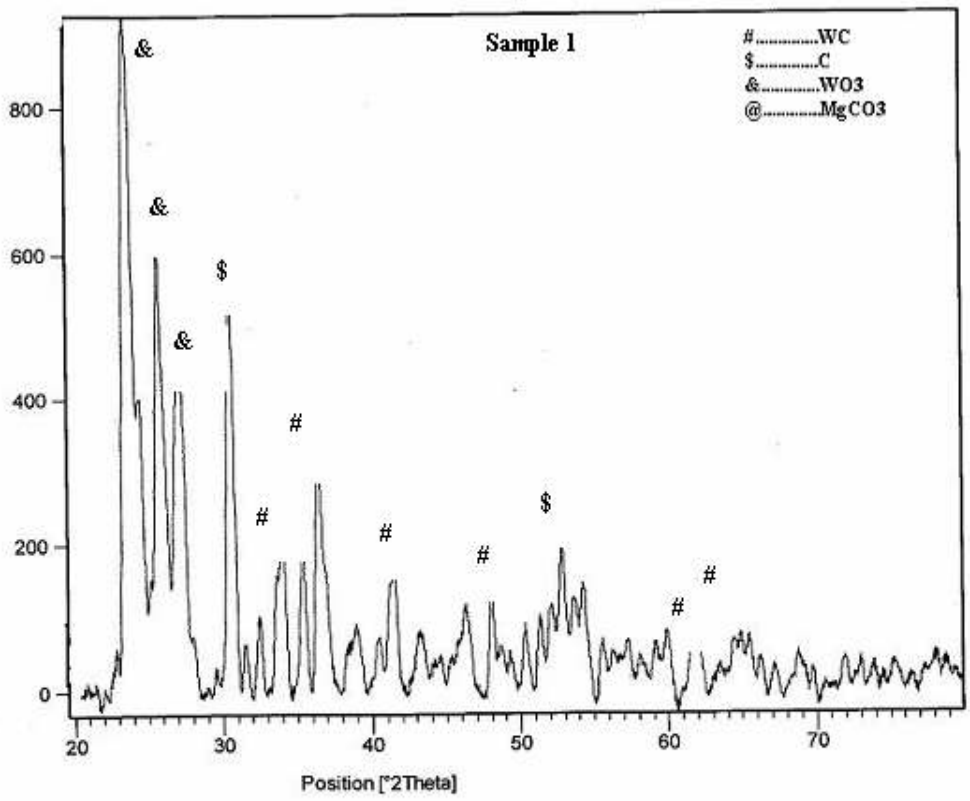

Fig 4.1 XRD Pattern for sample 1

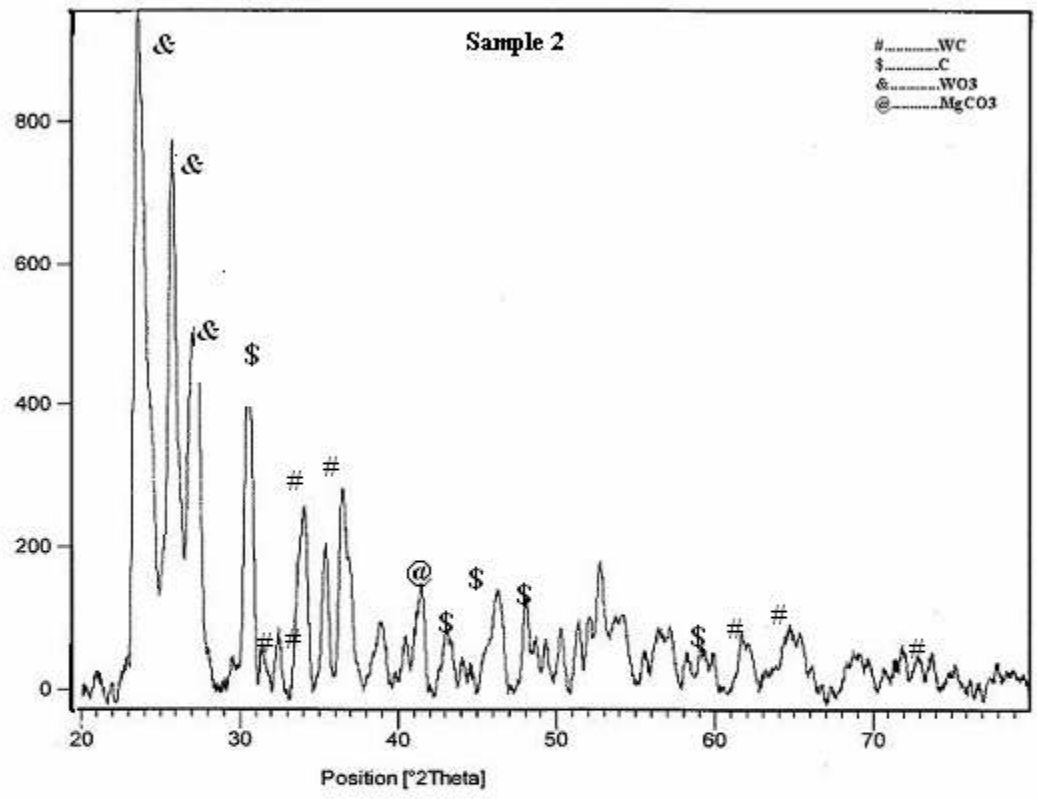

Fig 4.2 XRD Pattern for sample 2

4.2 Transmission Electron Microscopy Results

Transmission Electron Microscope results of the synthesized particles were done to know the particle size of synthesized powder which is present in fig 4.3- 4.12. The micrographs were taken from different regions. Looking at the features of micrograph it can be said that there are different types of phases which varies from spherical to elliptical, cylindrical to rectangular as can be seen in fig 4.4 and 4.5. the important features which were observed are that reaction is taking place where the powder is being encapsulated as can be seen in fig 4.7. Fig 4.6 represents the structure where facilitated morphology can be observed. The contrast variation observed in fig 4.6 is because of agglomeration of some of the particles and also because of existence of different phases. One of the important features which were observed is the high density of substance along the periphery of powder. Apparently it looks that carbon starts reacting with the substance and the excess carbon remaining at the periphery and being converted to the nano tube like structure.

As can be seen in Fig 4.8 once the reaction is over, the gelatinous compound which has found (Fig 4.8) burst leading to separation of other compounds where needle like structure and facilitated structure can be. Fig 4.9 reveals such type of morphology. The overall analysis indicates that during synthesis either gelatinous compound formed (Fig 4.8, 4.10,4.12). The overall structure gives complex type of phenomenon from which it can be concluded that reduction of WO_3 and high pressure is feasible. It is essential to optimize the magnesium properties by using different reducing reagents.

The X-ray analysis and TEM peaks indicated that the particles which are synthesized are with in the nanosize range. However, a detail analysis will reveal phases present in it.

Sample 1(1: 1 Acid Treated)


1.tif
Print Mag: 1040000x @ 7.0 in
20 nm

Fig 4.3

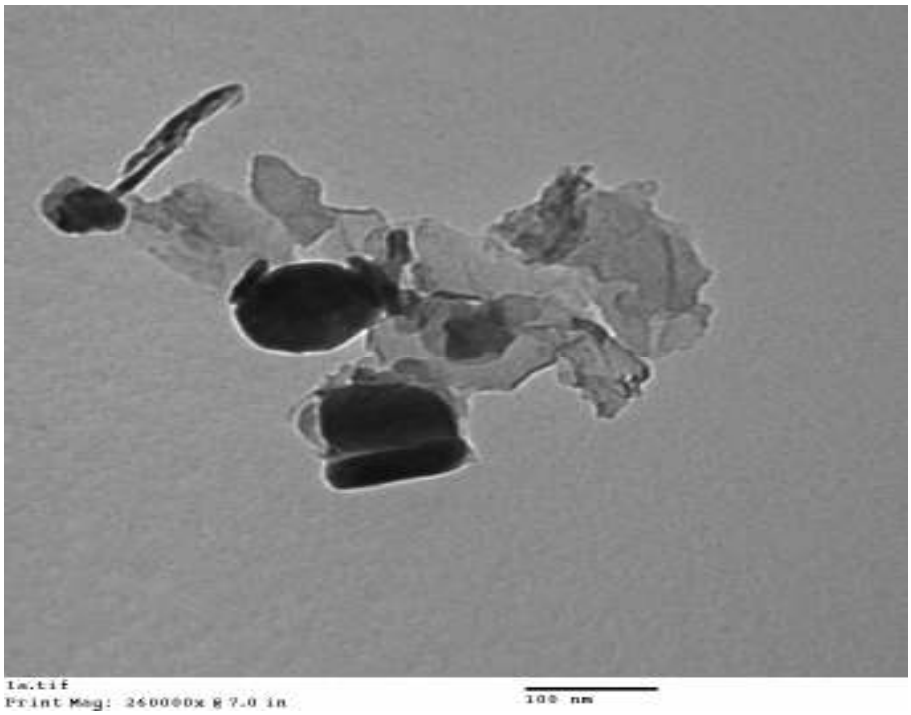
1m.tif
Print Mag: 260000x @ 7.0 in
100 nm

Fig 4.4

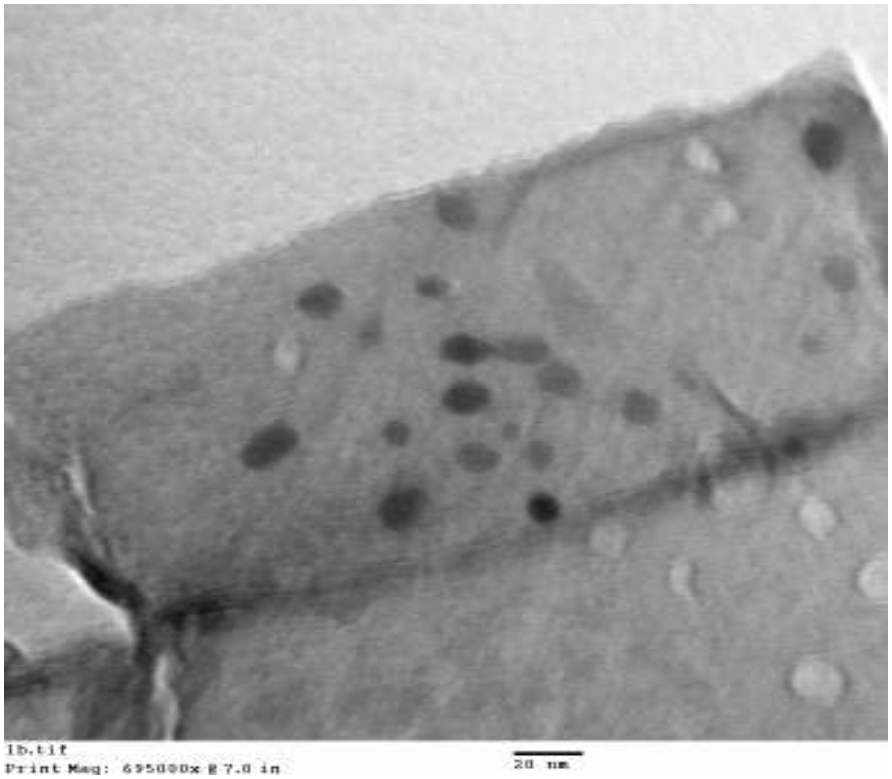
1b.tif
Print Mag: 695000x @ 7.0 in
20 nm

Fig 4.5

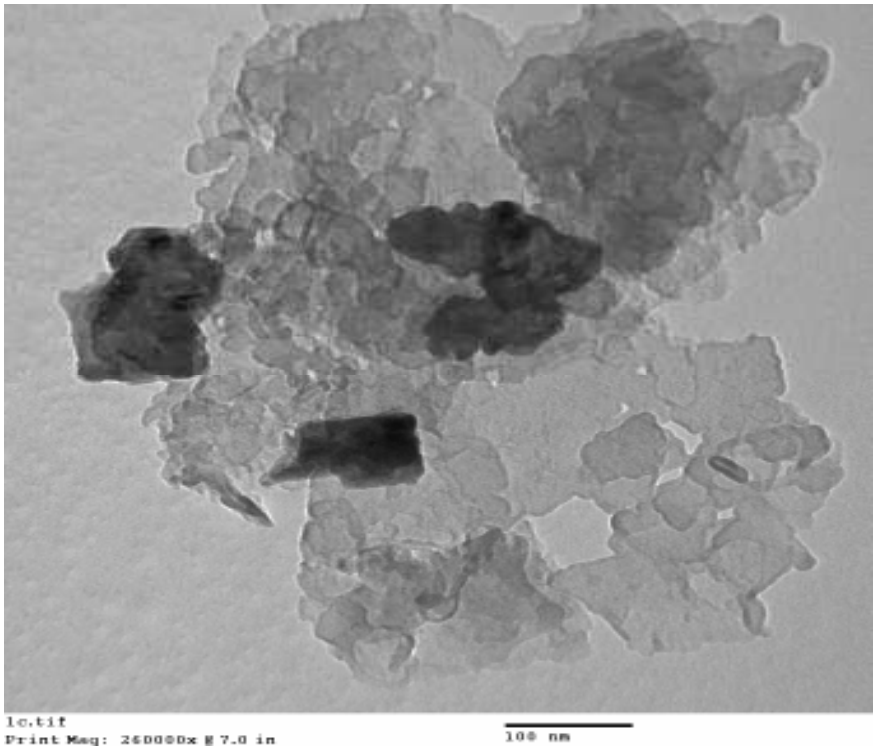
1c.tif
Print Mag: 260000x @ 7.0 in
100 nm

Fig 4.6

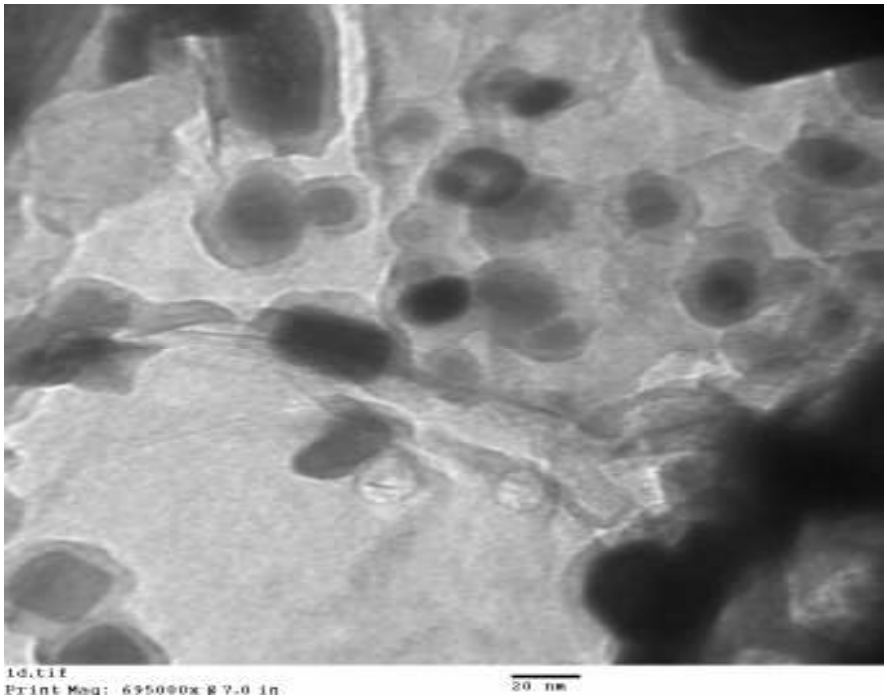

Fig 4.7

Sample 2 (Acid Treated 1:3)

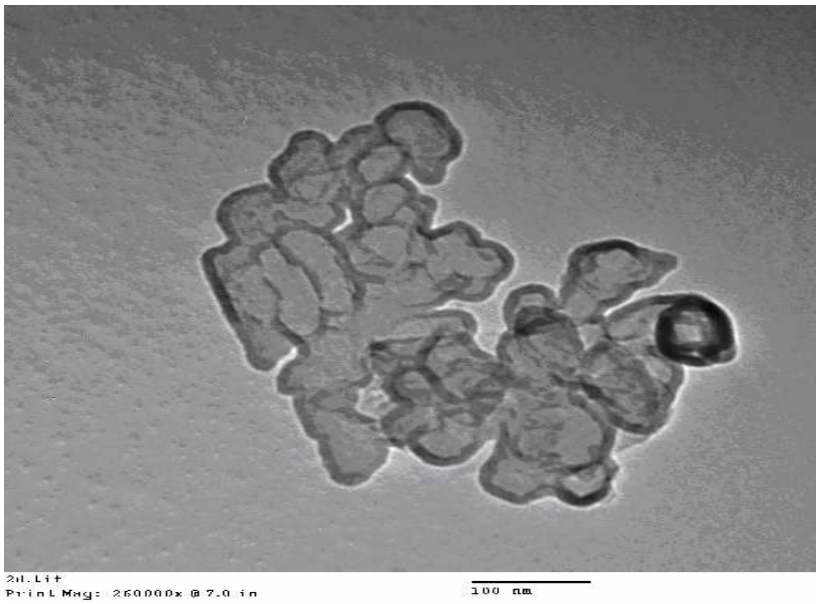

FIG 4.8

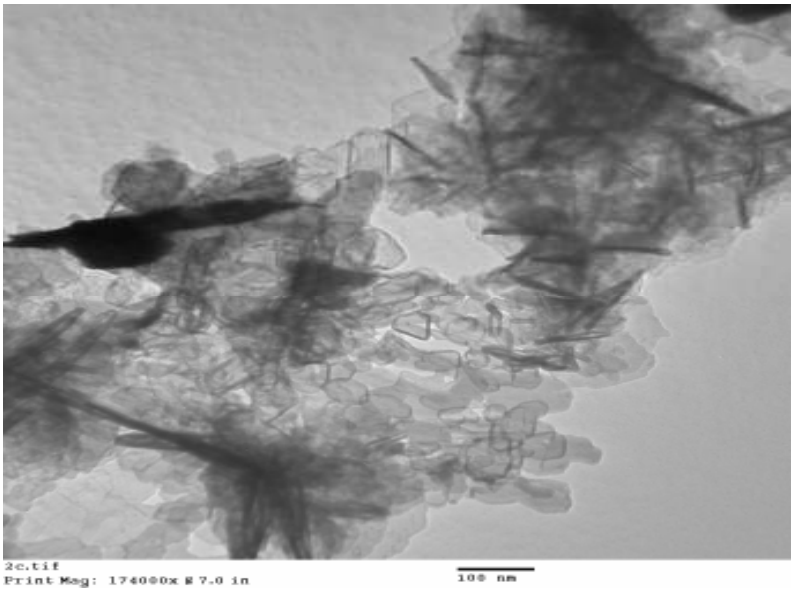

FIG 4.9

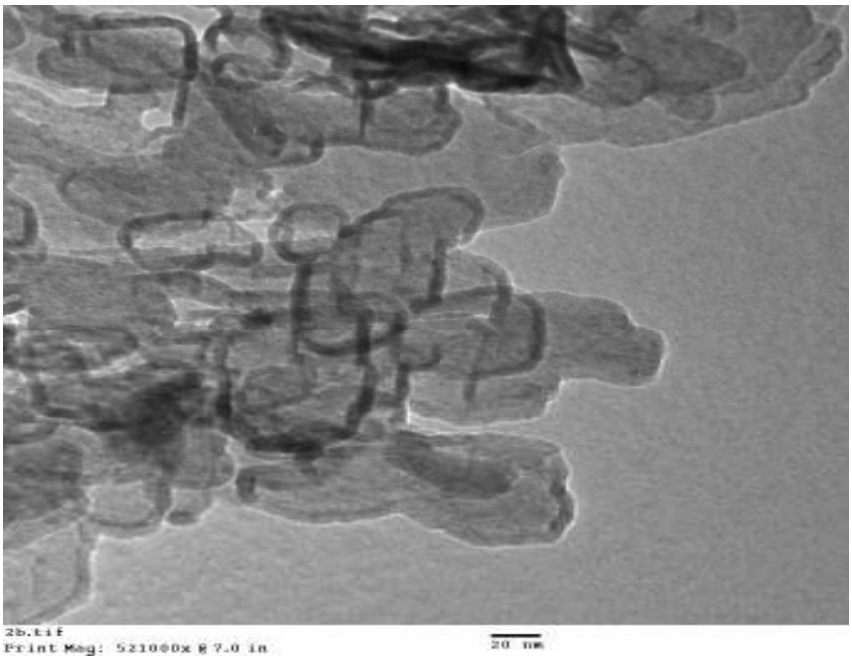

FIG 4.10

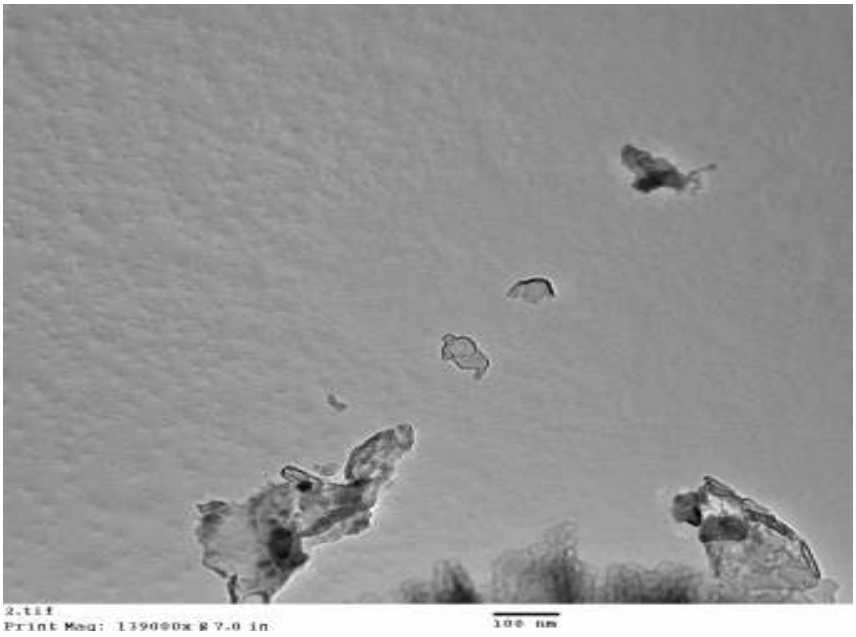

FIG 4.11

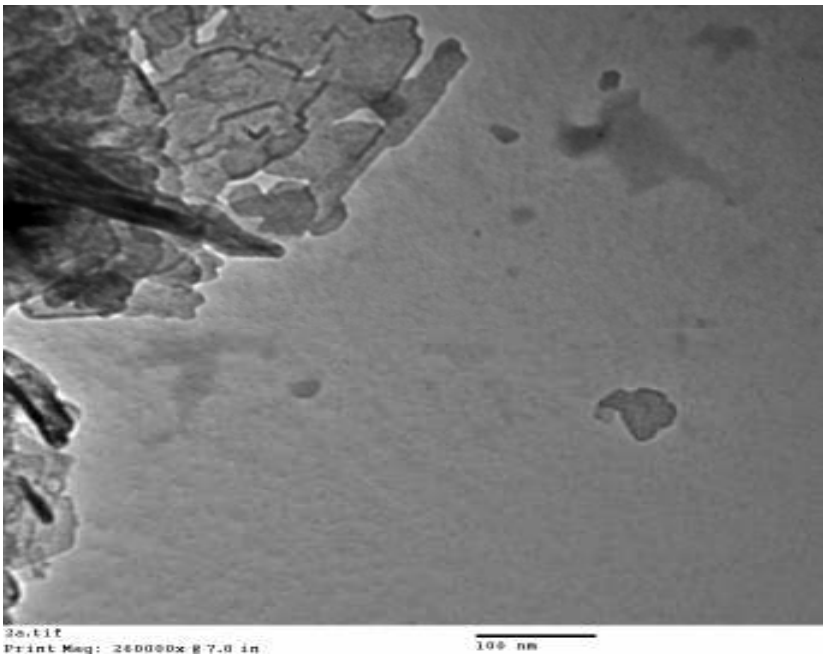

FIG 4.12

4.3 Differential Thermal Analysis Plots

Both the samples were examined by DTA/TGA to check their stability and phase transitions. The DTA/TGA plots of both the samples are shown in figure 4.5 and 4.6. The A (1) sample showed two exothermic peaks at 250 and 640°C. Apart from these peaks a weak endothermic peak was also observed at ~100°C. The broad peak at 640°C may be attributed to the combustion of the carboneous matter.

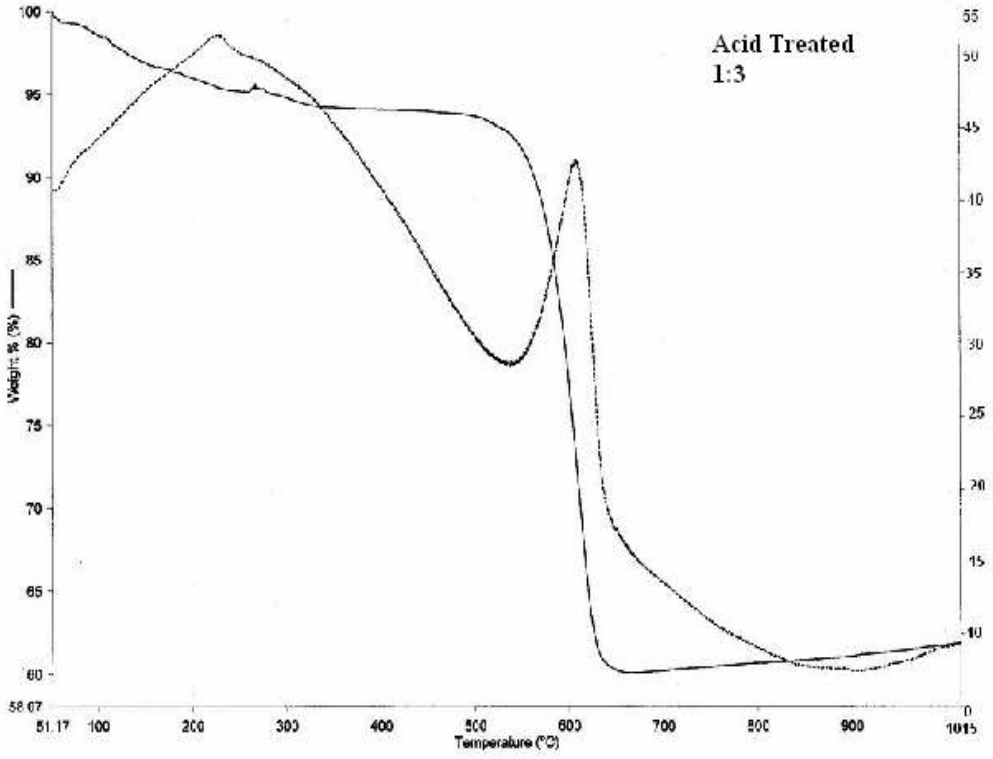

FIG 4.13 Sample (1)

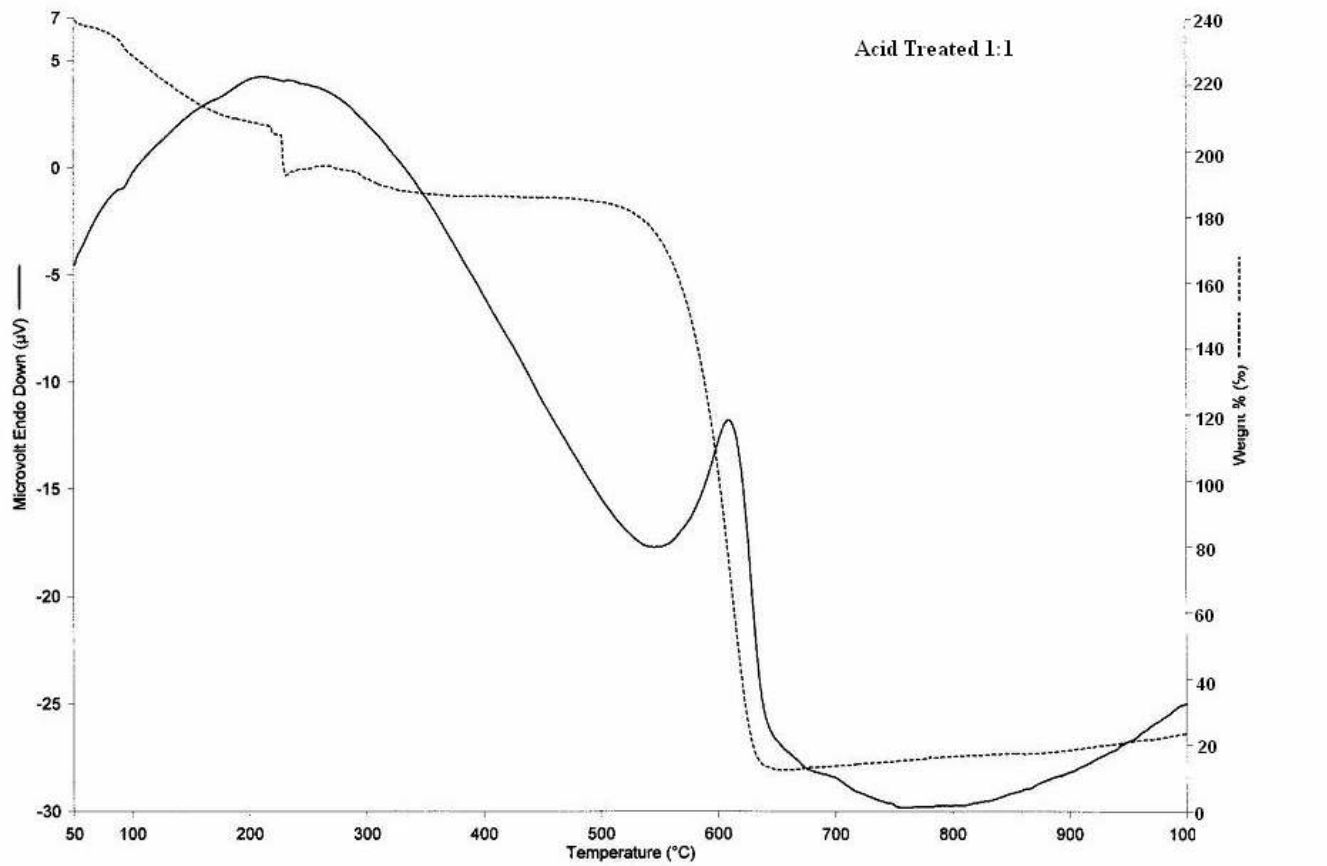

FIG 4.14 Sample (2)

The TGA plot of the samples shows weight loss. The weight loss of the samples clearly indicates that the carbon content in the samples. The DTA plot of A (2) sample showed more pronounced peaks at 250 and 620°C. At higher temperature a broad exothermic peak was observed at 620°C. The endothermic peak was observed at 100°C and 530°C.The TGA plot of the sample A (2) shows the weight loss at different temperatures.XRD peaks of carbon and weight loss in DTA/TGA analysis also showed that the carbon is in excess as compared to the other phases. Literature also propose the formation of the phases as discussed, but these phases can be leached out and we can get pure WC particles.

Chapter 5

Conclusions and Future Scope

In this study, it has been observed that thermo chemical route is one of the suitable techniques for the synthesis of WC nano particles. Since the process is low temperature synthesis (600-700º C) as compared to the other routes which has been followed for synthesis of WC nano particles, it makes the process more versatile.
From the present work, the following conclusions have been drawn:

1. It is possible to synthesize WC nano particles using organic solvent as source of carbon.
2. During synthesis several other phases has also formed which include W_2C, unreacted carbon and unreacted Mg compound.
3. It is possible to leach out other phases except carbon.
4. The phases which are present in synthesised powder show the possibility to synthesize WC nano particles of the suitable variation in process parameters.
5. Aromatic compounds as source of carbon have not shown good results but feasibility at high temperature exists.

Though this process leads to a complex reaction where the mechanism of transformation of WC to W_2C exists, it requires a lot of understanding as well as control over synthesis process.

REFERENCES

1. V.K.Sarin, "Cemented Carbide Cutting Tools", Advances in powder Technology. Ed. D. Y. Chin, ASM, **(**1981**)** pp. 253-287.
2. E. M. Trent, "Metal Cutting**"**, Butterworth's, Boston, 2nd Ed., 1984.
3. V. K. Sarin, "Cemented Carbide Cutting Tools", Advances in Powder Technology, Ed. D. Y. Chin, ASM, pp. 253-287, 1981.
4. "Tungsten", McGraw-Hill Encyclopaedia of Science and Technology, 7th Ed. 1992.
5. H. Kolaska, "The Dawn of the Hardmetal Age", Powder Metallurgical International, v24, no. 5, p 311-314, 1992**.**
6. 7. T. B. Massalski (Ed.), "Binary Alloy Phase Diagrams", Vol. 1: Alloys; Vol. 2: Phase Diagrams. ASM Int., Materials Park, Ohio, 1990.
7. R. Telle, "Boride and Carbide Ceramics", in Structure and Properties of Ceramics", Vol. 11, Ed. M. V. Swain, VCH, New York, 1994.
8. V. H.Hartmann, F. Ebert, O. Bretschneider, Z. Anorg.Allg. Chem., (1931) 198, 116
9. E. A Brandles , "Smithels Metal Reference Book", 6th Ed. Butterworth's, Boston, 1983
10. K. Scherer, US Patent 1,549,615 (application Oct. 31, 1923; patented 1925).
11. P. Schwarzkopf, Deutsche Edelstahlwerke, AG German Patent 720,502 (patented 1929, issued 1942).
12. A. E. McHale, "Phase Equilibria Diagrams – Phase Diagrams for Ceramists", Vol. 10, Fig. 8969, the American Ceramic Society, Westerville, Ohio, 1994.
13. H. J. Scussel, "Friction and Wear of Cemented Carbides", ASM Handbook, Vol. 18, ASM Int., pp. 795, 1992.
14. R. Dagani, "Nanostructured Materials Promise to Advance Range of Technologies", Chemical & Engineering News, Nov. 23 1992, 18-24
16. H. J. Scussel, "Friction and Wear of Cemented Carbides", ASM Handbook, Vol. 18, ASM Int., pp. 796, 1992.

17 P. Seegopaul and L. E. McCandlish, "Nanostructured WC-Co Powders: Review of Application, Processing and Characterization Properties", Adv. Powder Metall. Part. Mater. 3, 13/3-13/15, 1995.

18. J. J. Stiglich, C. C. Yu and T. S. Sudarshan, "Synthesis of Nano WC/Co for Tools And Dies", Tungsten Refract. Met. 3-1995, Proc. Int. Conf., 3rd 1995 (Pub. 1996), 229-236.

19. N C. Angastiniotis, B.H. Kear, L.E. McCandlish, K.V. Ramanujachary, M. Greenblatt, "Formation and Alloying of Nannostructured β-W Powders", Nanostructured Materials, Vol. 1, (1992) pp. 293-302

20. A. T. Santhanam, P. Tierney, and J. L. Hunt, "Cemented Carbides", Metals Handbook, ASM Int., Vol. 2, 10th Ed. pp. 950-977, 1990.

21. L. Zhang and T. E. Madey, "Initial Stages of Sintering of Nanostructured WC-7wt. %Co", NanoStructured Materials, 2, 487-493, 1993.

22. L.E. McCandlish, B.H. Kear and B.K Kim " Chemical Processing and properties of nanostructured WC-Co Materials(1992) Vol 1, pp. 119-124

23. Y. T.Zhu and A. Manthiram "Influence of Processing Parameters on the Formation of WC- Co Nanocomposite Powder Using a Polymer as Carbon Source". (1996) 407.

24. L.Geo and B.H. Kear "Synthesis of Nanophase WC Powder by a Displacement Reaction Process". Nanostructured Materials. Vol. **9**, pp 205-208, 1997

25. Z. G BAN. and L.L Shaw., "Synthesis and Processing of Nanostructured WC-Co Materials". Journal of Material Science**.** 37 (2002) 3397- 3403

26. J. Michael Hudson, W. John Peckett, and J.F. Peter Harris. "Low – Temperature Sol-Gel Preparation of Ordered Nanoparticles of Tungsten Carbide/ Oxide", Ind. Eng. Chem. Res. 2005, 44, 5575-5578.

27. B.S.Terry and D. C. Azubike, "Reduction- Carburization of Wolframite ($FeWO_4$):Part1- Reduction of Natural Wolframite Concentrate," Trans Inst. Mineral. Metall. (Sect.C: Mineral Process. Extr. Metall.), 99(1990**)**, 167-74

28. Chunli Guo, Lio Yi, Xiaojian Ma, Yitai Qian, and Liqiang Xu. "Synthesis of Tungsten Carbide Nanocrystal via a Simple Reductive Reaction". Chemistry Letters Vol. 35 No. 11 **(2006)**